Biogeosciences, 23, 3387–3406, 2026
https://doi.org/10.5194/bg-23-3387-2026

Biogeosciences Open Access EGU

Future mercury levels in fish: model vs. observational predictions under different policy scenarios

Henna Gull[1], Ju Hyeon Lee[2], Hoin Lee[1], Hélène Angot[3], and Sae Yun Kwon[1]

[1]Division of Environmental Science and Engineering, Pohang University of Science and Technology, 77 Cheongam-Ro, Nam-Gu, Pohang 37673, South Korea
[2]Harvard John A. Paulson School of Engineering and Applied Sciences, Harvard University, Cambridge, MA 02138, United States
[3]Univ. of Grenoble Alpes, CNRS, INRAE, IRD, Grenoble INP, IGE, 38400 Grenoble, France

Correspondence: Sae Yun Kwon (saeyunk@postech.ac.kr)

Received: 6 February 2026 – Discussion started: 24 February 2026
Revised: 23 April 2026 – Accepted: 30 April 2026 – Published: 20 May 2026

Abstract. Mercury (Hg) poses a global threat due to its long-range transport and transformation into methylmercury (MeHg), a potent neurotoxin that bioaccumulates in aquatic food webs. While global and regional efforts to reduce anthropogenic Hg emissions are ongoing, the implications of these policies for future Hg deposition and consequent MeHg levels in fish remain uncertain. This study synthesizes published modeling studies to examine projected relationships among Hg emissions, atmospheric deposition, and lake fish MeHg concentrations by 2050 under various policy scenarios. While models reveal a strong linear relationship between emissions and deposition ($R^2 = 0.79$), and a moderate correlation between Hg deposition and fish MeHg ($R^2 = 0.63$), these trends contrast with observational data, which often show nonlinear or more complex responses. Our analysis suggests that these relationships are partly shaped by shared structural assumptions within current modeling frameworks, particularly the treatment of atmospheric deposition as the dominant driver of future fish MeHg change and the representation of relatively short response times between changing Hg inputs and fish exposure, with limited representation of the time-lagged buffering provided by legacy Hg stores. Within these constraints, atmospheric deposition and lake area emerged as key predictors, with higher deposition and smaller lakes associated with higher modeled fish MeHg levels. Notably, despite wide variation in model structures, including differences in atmospheric chemistry, emission inventories, and food web dynamics, these linear trends persisted. By identifying these consistent patterns and the assumptions that support them, this study provides a benchmark for integrating currently underrepresented processes such as ecological complexity and climate-driven ecosystem feedbacks, into future assessments supporting the Minamata Convention.

1 Introduction

Mercury (Hg) occurs naturally in both inorganic and organic forms in the environment. Natural contributions include volcanic emissions, geothermal activity, and biomass burning (Kumar et al., 2018; Kumar and Wu, 2019), whereas anthropogenic sources are dominated by gold mining, coal combustion, metal production, cement manufacturing, and waste incineration (Pacyna et al., 2006; Pirrone et al., 2010; Rafaj et al., 2013). In addition to these sources, surface re-emissions from ocean and land reservoirs, including legacy emissions, amplify present-day atmospheric Hg burdens (Gustin et al., 2008; Pirrone et al., 2010; Gworek et al., 2020). Accounting for both historical anthropogenic inputs and their continued re-emission, current atmospheric Hg concentrations are estimated to be approximately 450 % higher than pre-1450 (pre-industrial) levels, accompanied by an average 300 % increase in global Hg deposition and a 230 % increase in surface ocean Hg concentrations (Outridge et al., 2018). This enrichment is spatially uneven, with atmospheric Hg levels increasing by up to 1600 % in the Northern Hemisphere and up to 400 % in the Southern Hemisphere relative to pre-industrial

levels (Li et al., 2020). In the atmosphere, Hg primarily exists as gaseous elemental Hg (GEM or Hg0), gaseous oxidized Hg (GOM or HgII), and particulate-bound oxidized Hg (PHg) (Kim and Zoh, 2012). GEM has a long atmospheric lifetime (0.5 to 1 year) due to its low solubility and relative chemical stability, enabling long-range transport (Selin, 2009; Ariya et al., 2015), whereas GOM is more soluble and reactive, with a lifespan of days (Moore et al., 2013). GEM was traditionally thought to be removed mainly through oxidation to GOM, which, along with PHg, is deposited via wet and dry pathways (Kim and Zoh, 2012). However, recent findings indicate that direct foliar and soil uptake of GEM accounts for 75 % of atmospheric Hg deposition to terrestrial surfaces (Obrist et al., 2018; Sonke et al., 2023).

Once deposited into aquatic ecosystems, inorganic Hg can be converted into methylmercury (MeHg), a potent neurotoxin (Gilmour et al., 2013). This process, facilitated by microbial activity, occurs in anoxic-suboxic sediments (Dai et al., 2021; Chen et al., 2025; Zhou et al., 2025) and within the water column of lakes (Capo et al., 2023; Peterson et al., 2025), estuaries (Bradford et al., 2023; Liu et al., 2023), and the open ocean (Sun et al., 2020; Zhang et al., 2020). As MeHg enters aquatic food webs, it bioaccumulates through both bioconcentration (direct uptake) and biomagnification (trophic interactions), posing risks to fish and humans consuming fish (Al-Sulaiti et al., 2022; Basu et al., 2023). While aqueous MeHg concentrations are reliable predictors for fish Hg levels (Wu et al., 2021; Blanchfield et al., 2022), these concentrations are shaped by complex interactions beyond direct atmospheric Hg input. For example, fish MeHg levels may vary more strongly with watershed or riverine Hg inputs than with atmospheric deposition (Willacker et al., 2020; Emmerton et al., 2023). Parameters such as lake size, morphology, and physicochemistry of water (pH, conductivity, dissolved organic carbon (DOC), nutrients) can also alter MeHg production and biotic uptake (Bodaly et al., 1993; Kidd et al., 2012; Ahonen et al., 2018; Knott et al., 2020; Ogorek et al., 2021). Beyond local conditions, climatic and ecological processes, including permafrost thaw, sea ice loss, food web shifts, and changing primary production, can substantially modify MeHg exposure in aquatic food webs (Wang et al., 2019; Lepak et al., 2019; Schartup et al., 2019; Schaefer et al., 2020; Y. Zhang et al., 2021). These combined influences highlight the complex, multi-scale drivers of Hg bioaccumulation in aquatic ecosystems.

Recognition of Hg's global transport and multifaceted drivers has spurred international regulation. Early actions included the 1998 Convention on Long-Range Transboundary Air Pollution Protocol on Heavy Metals, which targeted reductions in industrial Hg, cadmium (Cd), and lead (Pb) emissions from major sources and combustion processes (Selin and Selin, 2006). Reports by the Arctic Monitoring Assessment Program (AMAP) and the United Nations Environment Programme (UNEP) emphasized the need for global cooperation, complemented by European Union measures such as the 2005 Community Strategy Concerning Hg (Russ et al., 2009). The Minamata Convention on Hg, in force since 2017, now coordinates global efforts to reduce anthropogenic Hg emissions and releases across all sectors (Bank, 2020).

Over the years, projections of future Hg emission scenarios have been meticulously crafted through assessments of influencing factors (socio-economy, technology), and by employing diverse modeling techniques (Streets et al., 2009; Pacyna et al., 2016; Brocza et al., 2024; Geyman et al., 2024). In many atmospheric Hg modeling frameworks, emission inventories primarily represent anthropogenic sources, while natural and legacy re-emissions from land and ocean reservoirs are treated as separate fluxes within the model system (Corbitt et al., 2011). In several studies, these natural and legacy fluxes are prescribed as constant emissions based on historical deposition rather than responding dynamically to climate-driven changes (Corbitt et al., 2011; Giang et al., 2015). However, some recent frameworks couple atmosphere–ocean–land Hg cycling and allow legacy Hg in soils and oceans to respond to climate-driven changes in temperature, precipitation, and ocean circulation, thereby linking anthropogenic emission trajectories with climate-sensitive re-emissions in future projections (H. Zhang et al., 2021).

Estimating future Hg emissions and their impacts on ecosystem and fish Hg levels requires consideration of evolving socio-economic and technological drivers, atmospheric chemistry, biogeochemical processes, climate variability, land-use change, and ongoing emissions and re-emissions from legacy sources. This complexity has led to diverse modeling approaches, from simple to integrated frameworks with varying process representation. For example, D-MCM models link atmospheric deposition, in-lake cycling, and bioenergetic food webs, but simplify watershed inputs and use fixed trophic groups (Vijayaraghavan et al., 2014). Similarly, BASS-based coupled models simulate loading and bioaccumulation, yet retain simplified watershed export and food-web dynamics with limited treatment of legacy Hg, DOC, and ecological variability (Knightes et al., 2009). More recent non-steady-state models, such as SERAFM-derived frameworks, incorporate hydrology and water–sediment interactions but still estimate fish Hg using bioaccumulation factors, limiting representation of trophic dynamics and lags. Notably, most lake models link watershed export directly to atmospheric deposition, without explicit representation of soil Hg storage or legacy release (Perlinger et al., 2018).

This study revisits previously developed Hg emission scenarios formulated under varying policy frameworks and their modeled deposition (atmospheric chemistry–transport models) and impacts on fish MeHg (bioaccumulation models) to evaluate how policy-driven emission changes influence projected 2050 deposition patterns and lake fish MeHg, and the extent to which lake-specific characteristics mediate these relationships. We hypothesize that future emission changes may produce non-linear responses in Hg deposition, reflecting differences among models in spatial resolution, emission

inventories, meteorological drivers, and atmospheric chemistry. Deposition changes may further translate non-linearly to fish MeHg due to variability in bioaccumulation model structures and ecosystem-specific controls, which are often shaped by interacting environmental and climate-driven processes rather than by emissions alone (Burke et al., 2023; Gillies et al., 2024). Using published data and statistical analyses, we examine how prior future assessments simulate Hg deposition and bioaccumulation under varying policies and lake-specific effects.

2 Methodology

A total of 10 peer-reviewed studies were selected for analysis of projected anthropogenic Hg emissions, atmospheric deposition, and fish MeHg concentrations under 15 policy scenarios extending to 2050. Published between 2008 and 2025, these studies were identified through a targeted literature review and selected based on their ability to quantify at least two linked components of the Hg pathway: emissions and deposition, deposition and bioaccumulation, or all three using scenario-based modeling frameworks. Studies addressing only a single component were excluded. Studies examining the relationship between Hg emissions and atmospheric deposition are available across multiple geographic scales (e.g., global, regional, or local), and these were included to capture the broader range of modeled emission–deposition responses across different regions and modeling frameworks. In contrast, studies linking scenario-based Hg deposition projections to fish MeHg responses, using coupled atmospheric chemistry–transport and aquatic bioaccumulation models, are more limited and are primarily available for U.S. freshwater ecosystems, particularly lake systems. Accordingly, the deposition–MeHg analysis focuses mainly on several U.S. states (Maine, New Hampshire, Michigan, Florida, North Carolina, South Dakota, and Georgia), as shown in Fig. 1 and summarized in Table 2. This limitation reflects the availability of published model outputs rather than inherent constraints of the bioaccumulation models themselves; although these models can be parameterized for other regions, their application requires detailed local ecological, hydrological and biogeochemical input data that are not widely available.

Across the selected studies, diverse emission inventories, policy frameworks, and modeling approaches are used to simulate Hg pathways from emissions to ecosystem response. Scenario-based Hg emissions were first projected using global and/or regional inventories that differed in baseline year, emission source coverage, and assumed policy actions. These emissions served as inputs to atmospheric chemical transport models including GEOS-Chem, GLEMOS, ECHMERIT, and CAM-Chem/Hg (Lei et al., 2014; Pacyna et al., 2016; H. Zhang et al., 2021), to estimate spatial patterns of future Hg deposition. The modeled deposition outputs were subsequently coupled with aquatic bioaccumulation models such as BASS, D-MCM, and SERAFM (Knightes et al., 2009; Vijayaraghavan et al., 2014; Angot et al., 2018), to predict MeHg concentrations in fish. This sequential framework, from emissions to deposition to bioaccumulation, formed the foundation for the correlation and regression analyses conducted in this study. Comprehensive descriptions of the emission scenarios and modeling frameworks are provided in the Results and Discussion (Sect. 3.1 and 3.2) to support interpretation of results.

A detailed evaluation was also conducted of the models used to simulate Hg deposition and fish MeHg bioaccumulation, with emphasis on emission inventories, atmospheric transport mechanisms, biogeochemical processes, and methylation dynamics. Key variables, including emission scenarios, base years, global anthropogenic Hg emissions in the base year and in 2050, percentage change in deposition by 2050, atmospheric models, percentage change in fish MeHg by 2050, bioaccumulation model, study region, fish species, and references were systematically compiled using a pre-designed Excel spreadsheet. Since this study synthesizes previously published projections for 2050, the evaluation represents a comparative assessment of model frameworks and outputs rather than a direct statistical comparison with observational datasets, which is therefore a limitation of the present analysis. All extracted data and references are summarized in Tables 1, 2, S1, S4, and S7.

Our study employed Pearson correlation and regression analyses to investigate how changes in global anthropogenic Hg emissions under various policy scenarios relate to variations in Hg deposition by 2050. Statistical significance was assessed at the 95 % confidence level ($p < 0.05$). Changes in Hg deposition (% yr^{-1}) and changes in fish MeHg (% yr^{-1}) were evaluated for a subset of emission scenarios for which MeHg data were available. The formula used to calculate annual percent change in emissions, deposition, and fish MeHg is provided in Sect. S1. Multiple linear regression models (MLRMs) were first used to test whether lake characteristics, including average depth, lake surface area, watershed area, and wetland percentage, could explain variation in projected changes in fish MeHg. These lake characteristics represent present-day physical attributes reported in the original studies and were not projected for 2050. To explore multivariate relationships among predictor variables, Principal Component Analysis (PCA) was conducted on standardized data using Python 3.12.13 within the Google Colab environment, employing the scikit-learn, pandas, NumPy, SciPy, and matplotlib packages. The analysis included lake characteristics as used in the MLRM, projected changes in Hg deposition (% yr^{-1}), and projected changes in fish MeHg (% yr^{-1}) for 2050, all within the framework of Hg deposition scenarios. PCA reduced dimensionality by consolidating explanatory variables into principal component (PC) scores. A biplot was generated to visualize variable contributions and correlations to the first two PCs, with color intensity indicating relative in-

https://doi.org/10.5194/bg-23-3387-2026

Table 1. Projected changes in global anthropogenic mercury emissions and atmospheric deposition by 2050 under different policy scenarios and modeling frameworks.

Base year	Global anthropogenic Hg emissions in base year ($Mg\,yr^{-1}$)	Global anthropogenic Hg emissions in 2050 ($Mg\,yr^{-1}$)	Change in total Hg deposition in 2050 w.r.t. base year (%)	Model used for deposition simulations	Regions analyzed	References
SRES: Special Report on Emissions Scenarios – an Intergovernmental Panel on Climate Change (Nakicenovic et al., 2000) framework that projects future emissions based on trajectories of energy use, fuel consumption, economic development, and technological change. The scenarios are grouped into four main families: A1, A2, B1, and B2.						
A1B: A subset of A1 where all energy sources are balanced (neither high fossil dominance nor full non-fossil). [A1: A future characterized by rapid economic and technological growth, with global population peaking mid-century.]						
2000	2190	4856	75 75	CAM-Chem/Hg	Eastern U.S. Western U.S.	Lei et al. (2014)
2005	1900	4300	21 30	GEOS-Chem	Global U.S.	Corbitt et al. (2011)
2010	1890	4900	87	GEOS-Chem + MITgcm + GTMM	Global	Y. Zhang et al. (2021)
2015	2500	4900	40	5-box geochemical model for Arctic + Global Box Model	Arctic	Chen et al. (2018), AMAP/UNEP (2018)
2005	1900	4300	37	GEOS-Chem	Great Lakes	H. Zhang et al. (2021)
A2: A fragmented, self-reliant world with high population growth, slow technological change, and regionally oriented development.						
2005	1900	3400	25	GEOS-Chem	Global	Corbitt et al. (2011)
2010	1890	3900	59	GEOS-Chem + MITgcm + GTMM	Global	Y. Zhang et al. (2021)
2006	2480	3900	12	CTM-Hg, TEAM, AERMOD	Mendums Pond, NH	Vijayaraghavan et al. (2014)
A1F1: subset of A1 ("Fossil-intensive") where future energy use remains heavily dependent on fossil fuels.						
2000	2190	5984	100 75	CAM-Chem/Hg	Eastern U.S. Western U.S.	Lei et al. (2014)
No policy: Assumes no new Hg or air-quality controls beyond those implemented by 2010, with continued coal combustion and limited emission-control expansion.						
2005–2006	2000	4140	30	GEOS-Chem	U.S.	Giang and Selin (2016)
B1: An environmentally sustainable, convergent world with service-based economies and clean, efficient technologies.						
2000	2190	2386	13 0	CAM-Chem/Hg	Eastern U.S. Western U.S.	Lei et al. (2014)
2005	1900	1900	1 −10 −22	GEOS-Chem	Global U.S. Northeast U.S.	Corbitt et al. (2011)
2005	1900	1900	−13	GEOS-Chem	Great Lakes	H. Zhang et al. (2021)

Table 1. Continued.

Base year	Global anthropogenic Hg emissions in base year ($Mg\ yr^{-1}$)	Global anthropogenic Hg emissions in 2050 ($Mg\ yr^{-1}$)	Change in total Hg deposition in 2050 w.r.t. base year (%)	Model used for deposition simulations	Regions analyzed	References
B2: A local sustainability-focused scenario with moderate growth and slower, diverse technological change.						
2005	1900	2200	7	GEOS-Chem	Global	Corbitt et al. (2011)
2006	2480	2630	−15	CTM-Hg, TEAM, AERMOD	Mendums Pond, NH	Vijayaraghavan et al. (2014)
Minamata: Global treaty scenario achieving major emission cuts via best available technologies and control measures across key Hg sources.						
2005–2006	2000	2270	5	GEOS-Chem	U.S.	Giang and Selin (2016)
NPS: Implementation of pledged global actions (e.g., Minamata, fossil-fuel phase-outs) achieving notable emission cuts by 2035. [CPS: Continuation of 2010 policies and controls without new Hg-specific or climate initiatives.]						
2010	1960	0	−14	GEOS-Chem + GBC Model	Global	Angot et al. (2018)
			26		Ahmedabad (India)	
			−55		Shanghai (China)	
			−13		South Pacific	
			−15		Eastern lakes, Maine (U.S.)	
2010	1890	1020	−28	GEOS-Chem + MITgcm + GTMM	Global	Y. Zhang et al. (2021)
Constant emissions: Assumes no change in anthropogenic Hg emissions by 2050 with respect to 2015						
2015	2500	2500	12	5-box geochemical model for Arctic + Global Box Model	Arctic	Chen et al. (2018), AMAP/UNEP (2018)
MFR: Most optimistic case with universal adoption of best available technologies for maximum emission reduction.						
2010	1890	300	−48	GEOS-Chem + MITgcm + GTMM	Global	Y. Zhang et al. (2021)
2010	2000	0	−24	GEOS-Chem + GBC Model	Global	Angot et al. (2018)
			−38		Ahmedabad (India)	
			−68		Shanghai (China)	
			−22		South Pacific	
			−26		Eastern lakes, Maine (U.S.)	

fluence. Scree and contribution plots were also used to assess the relative importance of each component and to identify the most influential drivers in the dataset. In one case, results from (Knightes et al., 2009) were interpolated to estimate fish MeHg levels for 2050 under a simulated 50 % reduction in Hg deposition. Study locations were georeferenced and mapped using QGIS 3.28.5 to depict spatial coverage.

3 Results and discussion

3.1 Global anthropogenic Hg emission scenarios and atmospheric deposition

Understanding the relationship between Hg emissions and deposition is essential for assessing future environmental risks and exposure pathways. Researchers have employed various atmospheric Hg models to project Hg deposition patterns under multiple emission scenarios, each with distinct atmospheric chemistry mechanisms, meteorological drivers, and varying assumptions regarding legacy emissions. In particular, numerous studies have projected global anthropogenic Hg emissions up to 2050, using different scenario frameworks (Tables 1–2) and emission inventories (Supporting Information: Table S1). The main differences between scenarios lie in the stringency of Hg control measures and the underlying socio-economic–energy trajectories – ranging from *minimal-control, high-growth futures* (A1F1, A1B, A2, CPS, Minimal-regulation, SSP5-8.5) (Knightes et al., 2009; Sunderland and Selin, 2013; Vijayaraghavan et al., 2014; Lei et al., 2014; Giang et al., 2015; Chen et al., 2018; Perlinger et al., 2018; H. Zhang et al., 2021; Schartup et al., 2022; Brocza et al., 2024; Geyman et al., 2024, 2025) with rising emissions, through *intermediate-policy pathways* (B1, B2, PIA, NPS, CLIM, Minamata, SSP5-3.4, SSP2-4.5) (Streets et al., 2009; Sunderland and Selin, 2013; Rafaj et al., 2013; Vijayaraghavan et al., 2014; Lei et al., 2014; Giang and Selin, 2016; Angot et al., 2018; Perlinger et al., 2018; H. Zhang et al., 2021; Y. Zhang et al., 2021; Geyman et al., 2024, 2025) that stabilize or moderately reduce emissions, to *maximum-mitigation futures* (50 % Reduction, MFR, CLIM + MFR, Aspirational, Zero emissions, Net Zero + MFR, SSP1-2.6) (Pacyna et al., 2016; Angot et al., 2018; Chen et al., 2018; Perlinger et al., 2018; Y. Zhang et al., 2021; Brocza et al., 2024; Geyman et al., 2024, 2025) achieving the deepest cuts. In some studies, e.g., (Giang and Selin, 2016), Minamata and No-Policy scenarios adopt B1- and A1B-type socio-economic assumptions, respectively. To illustrate their origins and policy focus, Figure S1 organizes these scenarios into four thematic families: Hg-focused policy scenarios, SRES-based frameworks, shared socioeconomic pathways, climate-oriented pathways, and hybrid syntheses. Collectively, these studies span the full spectrum from continued growth to deep global reductions in anthropogenic Hg emissions. The acronyms for Hg-focused and SRES scenar-

Table 1. Continued.

Base year	Global anthropogenic Hg emissions in base year ($Mg\,yr^{-1}$)	Global anthropogenic Hg emissions in 2050 ($Mg\,yr^{-1}$)	Change in total Hg deposition in 2050 w.r.t. base year (%)	Model used for deposition simulations	Regions analyzed	References
Hg Controls: Assumes 50% reduction in primary anthropogenic Hg emissions by 2050 via widespread Hg-specific controls.						
2015	2500	1250	−16	5-box geochemical model for Arctic + Global Box Model	Arctic	Chen et al. (2018), AMAP/UNEP (2018)
Zero Emissions: Idealized case where all primary anthropogenic Hg emissions cease after 2015, representing the maximum achievable reduction.						
2015	2500	0	−50	5-box geochemical model for Arctic + Global Box Model	Arctic	Chen et al. (2018), AMAP/UNEP (2018)

Table 2. Projected changes in atmospheric Hg deposition and corresponding fish MeHg concentrations by 2050 across different scenarios and modeling frameworks.

Base year	Change in total Hg deposition in 2050 w.r.t. base year (%)	Model used for deposition simulations	Change in MeHg in fish in 2050 w.r.t. base year (%)	Models used for MeHg in fish simulations	Regions analyzed	Fish type	References
SRES: Special Report on Emissions Scenarios – an Intergovernmental Panel on Climate Change (Nakicenovic et al., 2000) framework that projects future emissions based on trajectories of energy use, fuel consumption, economic development, and technological change. The scenarios are grouped into four main families: A1, A2, B1, and B2.							
SRES A2: A fragmented, self-reliant world with high population growth, slow technological change, and regionally oriented development.							
2006	12	CTM-Hg, TEAM, AERMOD	5	D-MCM	Mendums Pond, NH	LMB and yellow perch	Vijayaraghavan et al. (2014)
SRES B2: A local sustainability-focused scenario with moderate growth and slower, diverse technological change.							
2006	−15	CTM-Hg, TEAM, AERMOD	−14	D-MCM	Mendums Pond, NH	LMB and yellow perch	Vijayaraghavan et al. (2014)
NPS: Implementation of pledged global actions (e.g., Minamata, fossil-fuel phase-outs) achieving notable emission cuts by 2035. [CPS: Continuation of 2010 policies and controls without new Hg-specific or climate initiatives.]							
2010	−15	GEOS-Chem + GBC Model	−11	Hendrick's LMB model	Eastern lakes, Maine	Brook trout, brown trout, burbot, Landlocked salmon, and smallmouth bass	Angot et al. (2018)
Policy-in-action: Full implementation of existing Hg-control measures, including Minamata Convention and U.S. Clean Air Act rules, stabilizing emissions near current levels by 2050.							
2005–2006	−15	GEOS-Chem	−11	Hendrick's LMB model	Lakes in Michigan's UP	Northern pike, LMB, Yellow perch, and Pickerel	Perlinger et al. (2018)
	12		19		Lake in Michigan's UP with Adirondack's deposition	Walleye	
	12		−38		Lake in Michigan's UP with Adirondack's deposition and watershed features	Walleye	
MFR: Most optimistic case with universal adoption of best available technologies for maximum emission reduction.							
2010	−26	GEOS-Chem + GBC Model	−22	Hendrick's LMB model	Eastern lakes, Maine	Brook trout, brown trout, burbot, Landlocked salmon, and smallmouth bass	Angot et al. (2018)
Aspirational: Assumes complete elimination of anthropogenic Hg emissions by 2050 through a global transition to Hg-free technologies and renewable energy sources.							
2005–2006	−65	GEOS-Chem	−65	Hendrick's LMB model	Lakes in Michigan's UP	Northern pike, LMB, Yellow perch, and Pickerel	Perlinger et al. (2018)
Reduction in deposition, 50 %: A scenario applying a uniform 50 % reduction to locally observed Hg deposition (without specifying global emissions).							
2001	−50	Community Multi-scale Air Quality Model (CMAQ)	−31	WASP, SERAFM, BASS	Eagle Butte Lake, SD	Northern pike	Knightes et al. (2009)
			−51		Lake Barco, FL	LMB	
			−57		Pawtuckaway Lake, NH	yellow perch	
			−77		Lake Waccamaw, NC	LMB	
			−74		Brier Creek, GA	Pickerel	

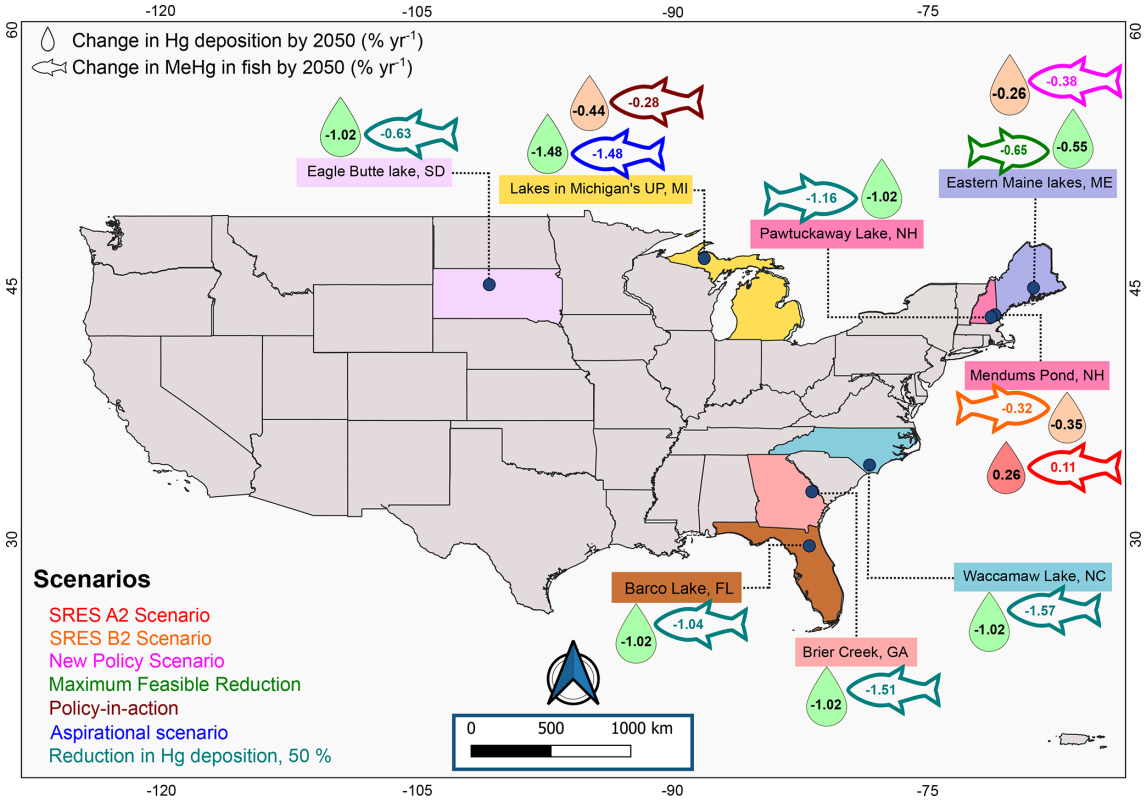

Figure 1. Geospatial distribution of projected changes in atmospheric Hg deposition and fish MeHg concentrations across the United States by 2050. Blue dots indicate study locations. Droplet symbols represent scenario-based changes in Hg deposition, while fish symbols show corresponding changes in fish MeHg. Fish colors denote emission policy scenarios: MFR and NPS (Angot et al., 2018), SRES A2 and B2 (Vijayaraghavan et al., 2014), Policy-in-action and Aspirational (Perlinger et al., 2018), and a uniform 50 % reduction in Hg deposition (Knightes et al., 2009). Droplet fill colors indicate relative emission (or deposition) levels across scenarios, classified as low (green), medium (orange), and high (pink).

ios are defined in Tables 1–2, while climate-oriented and hybrid frameworks, often reported only as emission trajectories and, in some cases, not extending to 2050 or lacking deposition outputs – are listed separately in Table S2.

These emission scenarios have been applied in a variety of atmospheric models, which differ in spatial resolution, redox chemistry, and meteorological drivers (Table S7). The oxidation of Hg^0, primarily by ozone (O3) and hydroxyl radicals (OH), is incorporated in several models, including HYSPLIT-Hg (Cohen et al., 2016), CAM-Chem/Hg (Lei et al., 2014), CTM-Hg (Vijayaraghavan et al., 2014), GLEMOS and ECHMERIT (Pacyna et al., 2016; De Simone et al., 2017; Travnikov et al., 2017). Some models, such as GLEMOS and GEM-MACH-Hg, also incorporate Br oxidation in polar regions, although GEM-MACH-Hg mainly relies on OH chemistry (Travnikov et al., 2017). The older version of GEOS-Chem simulated Hg^0 oxidation by Br and HgII photoreduction in clouds, following the mechanism proposed by (Holmes et al., 2010). (Horowitz et al., 2017) later refined this chemistry by introducing second-stage oxidation of HgBr by HO_2 and NO_2, based on the mechanisms of (Dibble et al., 2012) and (Shah et al., 2016). More recently, (Shah et al., 2021) proposed a revised mechanism where Hg^0 oxidation is driven by both Br and OH radicals, with O3 playing a secondary role. HgII is mainly reduced via photolysis of HgII-organic complexes and gas-phase HgI species. In addition, models employ distinct meteorological drivers, ranging from offline simulations forced by reanalysis or prescribed meteorological fields (e.g., GEOS-5, MERRA-2, ECMWF, CCSM in specified-dynamics mode, and NCEP/NCAR) (Bullock et al., 2009; Corbitt et al., 2011; Vijayaraghavan et al., 2014; Lei et al., 2014; Pacyna et al., 2016; Cohen et al., 2016; Travnikov et al., 2017; Angot et al., 2018) to fully online coupling with general circulation or weather prediction models (e.g., NASA GISS GCM ModelE2, ECHAM5, and GEM) (Travnikov et al., 2017; Y. Zhang et al., 2021; H. Zhang et al., 2021) (Table S7). These differences introduce additional variability in simulated atmospheric transport, oxidation, and deposition patterns. Models also rely on different anthropogenic and natural Hg emission inventories, further contributing to variability in projected deposition. Details of the inventories used in the models and the scenarios to which

they are coupled are provided in Table S1, while abbreviations for the meteorological drivers are listed in Table S7.

To assess the influence of changes in anthropogenic Hg emissions on future deposition, we analyzed the relationship between annual changes (% yr^{-1}) in global anthropogenic Hg emissions and corresponding annual changes (% yr^{-1}) in Hg deposition projected for 2050 (Fig. 2). Each data point represents a specific combination of atmospheric model, emission scenario, surface type, and region. For each case, the change in emission and deposition estimates are derived from the same study to maintain internal consistency within each scenario. The relationship is strikingly linear ($R^2 = 0.79$, slope = 0.41, $p < 0.001$), meaning that 79 % of the observed variability in Hg deposition is explained by changes in emissions. Yet the slope indicates that a 1 % change in emissions yields about a 0.4 % change in deposition, implying that a substantial fraction of emitted Hg undergoes chemical transformation and/or transport, while also reflecting the influence of re-emissions and the legacy mercury pool.

While these emission projections largely explain future Hg deposition trends, Fig. 2 also illustrates variability in annual changes (% yr^{-1}) in Hg deposition under the same scenarios. These differences, although relatively small, arise from variations in model configurations, including redox chemistry, spatial resolution, meteorological drivers, and treatment of legacy reservoirs. For instance, under the A1B scenario, (Corbitt et al., 2011) applied a coarse-resolution GEOS-Chem configuration with a simplified one-step Br oxidation scheme and static legacy pools, resulting in only a 0.46 % yr^{-1} increase in global Hg deposition (ellipse C, region 3). In contrast, (Y. Zhang et al., 2021) projected a much stronger 2.18 % yr^{-1} increase, reflecting the use of finer spatial grids, updated anthropogenic inventories, a two-step Br oxidation pathway, and fully coupled ocean-terrestrial reservoirs. Even in the relatively stable B1 scenario, where global anthropogenic emissions remain nearly constant, deposition projections for the U.S. diverge slightly. (Corbitt et al., 2011) projected a modest decrease in deposition, while (Giang and Selin, 2016) projected a slight increase (ellipse B, region 4). This contrast can be attributed to differences in model setup: (Corbitt et al., 2011) used a coarse $4° \times 5°$ global grid with fixed meteorology and treated biomass burning as part of the legacy pool, whereas (Giang and Selin 2016) applied a nested $0.5° \times 0.667°$ North American domain with updated emission inventories.

In addition to these differences, the treatment of historical emission inventories further contributes to uncertainty in modeled Hg deposition. While recent work by (Guerrero and Schneider, 2023) challenged previous overestimates of pre-industrial emissions by (Nriagu, 1993, 1994, Streets et al., 2009, 2011, 2017; Streets et al., 2019), they demonstrated that chemically sequestered forms of Hg (e.g., calomel, vermilion) were previously omitted or underestimated in historical emission inventories. Their findings, supported by (Engstrom et al., 2014) and (Outridge et al., 2018), indicate that pre-industrial emissions may have been 2–5 times lower than earlier estimates. However, (Angot et al., 2018) demonstrated that halving historical (1850–1920 CE) mining emissions had no significant impact on the projected benefits of delayed policy action, reinforcing the finding that atmospheric deposition is most sensitive to recent anthropogenic emissions. (Médieu et al., 2024) also emphasized the rapid responsiveness of the atmospheric Hg reservoir to emission changes, in contrast to the slower response of legacy reservoirs like the ocean.

Taken together, these results indicate that contemporary anthropogenic emissions overwhelmingly drive global Hg deposition in the model-simulated world, with diverse modeling frameworks converging on this conclusion despite differences in atmospheric chemistry, spatial resolution, treatment of legacy reservoirs, meteorological drivers, and uncertainties in historical emission inventories. However, an important question remains as to whether real-world systems respond as linearly as suggested by current models.

Model–observation inconsistencies are evident across multiple spatial scales. (Holloway et al., 2012) found that across 31 Mercury Deposition Network (MDN) sites in the Great Lakes region, the CMAQ-Hg model underestimated annual Hg wet deposition by about 21 % on average, with seasonal biases including underprediction in spring–fall and overprediction in winter (approx. 70 %). Similarly, MDN observations in the southeastern U.S. show that the global GEOS-Chem model ($4° \times 5°$) underestimated deposition by about 46 %, largely due to its inability to resolve deep convection, a key driver of Hg wet deposition (Xu et al., 2022). In China, observations indicate faster declines than models predict, with GEM decreasing by approx. 19 % compared to an 11 % modeled reduction over 2013–2017 (Feng et al., 2024; Liu et al., 2019).

Model-observation discrepancies are also apparent at the hemispheric scale. (Travnikov et al., 2017) evaluated four global Hg models (GLEMOS, GEOS-Chem, GEM-MACH-Hg, and ECHMERIT) against observations and found that performance depends strongly on oxidation chemistry and precipitation scavenging. Br-based schemes peak in spring, while OH-based schemes better capture North American and European summer peaks, indicating no single pathway fully explains observed patterns. Furthermore, in the Southern Hemisphere, GEOS-Chem and MITgcm overestimate wet deposition by approx. 5-fold and underestimate dry deposition by 3.5-fold relative to observations, reflecting simplified representations of convective uplift and precipitation scavenging (Leiva González et al., 2022).

Together, these discrepancies highlight the need for more routine and systematic comparisons between modeled and observed deposition trends under evolving policy conditions. Strengthening long-term monitoring networks and further harmonizing emission inventories will be essential to validate model predictions and to assess the real-world effective-

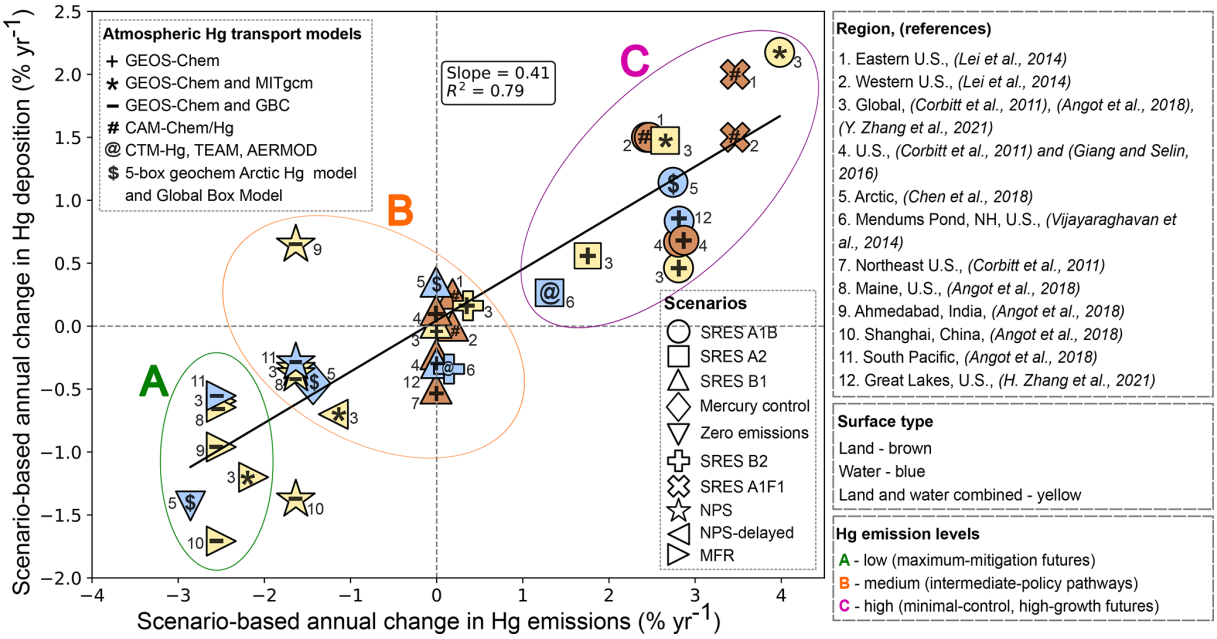

Figure 2. Relationship between scenario-based annual changes in global anthropogenic Hg emissions (% yr^{-1}) and corresponding changes in Hg deposition (% yr^{-1}) projected for 2050 across multiple models, regions, and policy scenarios. Marker shapes represent emission scenarios, while symbols indicate deposition models. Numbers correspond to regions and references (top right panel). Marker fill colors indicate surface types: land (brown), water (blue), and combined land–water (yellow). Ellipses indicate emission levels, with A (green) representing low emissions, B (orange) medium emissions, and C (pink) high emissions.

ness of Hg control measures under the Minamata Convention.

3.2 Relationship between Hg deposition and fish MeHg under future scenarios

Atmospheric deposition plays a pivotal role in biogeochemical cycling and fate of Hg in aquatic ecosystems. Studies have shown that atmospherically supplied Hg can rapidly be converted to MeHg in lake ecosystems and enter the base of the food chain, elevating fish MeHg levels within a short period (Harris et al., 2007; Ogorek et al., 2021). Understanding the relationship between atmospheric Hg deposition and MeHg concentrations in fish is essential for predicting future risks under varying emission scenarios, especially in the context of evolving policies.

To estimate MeHg concentrations in fish under future deposition scenarios, researchers have used multiple bioaccumulation models, including SERAFM, Hendrick's Lake Mass Balance Model, D-MCM, BASS, and WASP, as described below.

a. *SERAFM*: Spreadsheet-based Ecological Risk Assessment for the Fate of Hg model operates under steady-state conditions, estimating Hg concentrations in fish using bioaccumulation factors (BAFs). It employs a three-box system (epilimnion, hypolimnion, and sediments) to model Hg dynamics, incorporating atmospheric deposition of Hg0, MeHg, and HgII with same wet and dry deposition fluxes for lakes and watersheds. However, it does not account for Hg accumulation during ice cover and subsequent release during spring melt. Watershed inputs rely on constant runoff coefficients without seasonal variability, and erosion is modeled using the Revised Universal Soil Loss Equation (RUSLE). Seasonal changes in temperature, stratification, ice cover, and DOC inputs are not simulated, and rate constants for oxidation-reduction, photodegradation, and other processes remain fixed throughout the simulation (Knightes, 2008; Knightes et al., 2009).

b. *Hendrick's Lake Mass Balance Model*: A modified version of SERAFM, operates under non-steady-state conditions while still using BAFs for fish Hg estimation (Perlinger et al., 2018). It also employs a three-box reservoir system but distinguishes deposition between lakes and watersheds, incorporating higher friction velocities in watersheds (Angot et al., 2018). Unlike SERAFM, it accounts for accumulated deposition during ice cover and its release in spring melt. Seasonal dynamics in temperature, stratification, and ice cover are simulated, and DOC inputs follow a sine function to capture seasonal fluctuations. Rate constants for redox reactions, methylation, demethylation, and photodemethylation adjust dynamically based on lake temperature and light attenuation, while thermocline dispersion rates

vary seasonally to reflect mixing and stratification (Hendricks, 2018).

c. *D-MCM:* The Dynamic Mercury Cycling Model predicts time-dependent concentrations of Hg0, MeHg, and HgII across the water column, sediments, and a six-level food web, including phytoplankton, zooplankton, benthos, and three fish trophic levels (Zhu et al., 2018). It models dry and wet atmospheric deposition of HgII and MeHg, while incorporating processes such as adsorption, desorption, particulate settling, sediment-water exchange, resuspension, burial, air-water gaseous exchange, and in-situ transformations in lakes (Massoudieh et al., 2010). Bioenergetics influence MeHg accumulation by linking fish metabolism, feeding, and growth to Hg uptake and retention. In the model, higher activity costs or lower growth efficiency result in higher MeHg concentrations, highlighting how fish allocate consumed energy between growth and activity and its effect on Hg burden (Harris and Bodaly, 1998; Trudel and Rasmussen, 2006). However, like SERAFM, D-MCM does not account for Hg accumulation during ice cover and its subsequent release. Watershed inputs rely on time series data of precipitation and Hg concentrations, with constant MeHg assumptions in precipitation. Surface flow rates are modeled using constant runoff coefficients (Vijayaraghavan et al., 2014).

d. *BASS:* The Bioaccumulation and Aquatic System Simulator explicitly models Hg uptake in fish through dietary ingestion and gill exchange, rather than relying on BAFs. Hg levels are moderated by metabolic elimination, which removes Hg, and growth dilution, which reduces MeHg concentrations (Barber, 2008). BASS incorporates age-structured fish populations, covering both small, short-lived species and large, long-lived species, while allowing simulation of diverse fish communities based on species-specific physiological and ecological parameters, including dietary composition and growth patterns. It also models food web interactions by simulating biomass changes in phytoplankton, zooplankton, and benthos due to consumption, respiration, and mortality (Barber, 2018). However, BASS does not simulate external Hg inputs, such as those from atmospheric deposition, watershed runoff, or upstream river inflows. Instead, it requires the user to provide initial Hg concentrations in water and biotic compartments (e.g., plankton, benthos) (Knightes et al., 2009; Barber, 2018). These concentrations are typically estimated from field measurements or generated by external models such as the Watershed Characterization System Hg Loading Model (WCS-MLM) (Greenfield et al., 2002) and SERAFM. Additionally, BASS lacks capabilities for modeling Hg deposition, transport, transformation, and fate within aquatic systems, requiring integration with models such as SERAFM and WASP (Knightes et al., 2009).

e. *WASP:* The Water Analysis Simulation Program (WASP) supports both steady-state and non-steady-state simulations, utilizing a four-layer system that includes the water column, mixed sediment, methylation layer, and deep sediments (Vuksanovic et al., 1996). The model receives atmospheric deposition inputs of Hg0, HgII, and MeHg but focuses solely on in-waterbody processes, relying on external models for watershed Hg fluxes (Lindenschmidt, 2006). Hg transformations in WASP are compartment-specific: methylation occurs primarily in the anaerobic sediment methylation layer, while demethylation, oxidation, and reduction occur in both the surface water and in the aerobic mixed sediment layer (Gidley et al., 2017). WASP does not simulate sediment resuspension processes directly; these must be estimated separately. Seasonal drivers like temperature variation, stratification, and ice cover are not incorporated into the model (Knightes et al., 2009).

To assess how changes in atmospheric Hg deposition influence fish MeHg concentrations, we analyzed the relationship between annual changes (% yr^{-1}) in atmospheric Hg deposition and corresponding changes (% yr^{-1}) in fish MeHg projected for U.S. ecosystems by 2050 (Fig. 3). Each point integrates atmospheric and bioaccumulation models, fish trophic levels, sites, and emission scenario-based deposition. Deposition and fish MeHg changes are derived from the same study, ensuring internal consistency. Despite the diversity of atmospheric models, bioaccumulation frameworks, fish species, and ecosystem types represented, the relationship is strongly linear ($R^2 = 0.63$, slope $= 0.87$, $p < 0.01$), indicating that roughly 63 % of the variance in the projected change of fish MeHg is explained by scenario-based changes in atmospheric Hg deposition. The slope shows that every 1 % change in deposition yields an approximately 0.87 % change in fish MeHg, a far steeper response than the 0.4 slope found for emissions versus deposition (Fig. 2). This suggests that fish incorporate nearly all deposited Hg into food webs in the model-simulated world. However, the correlation is weaker than that observed between emissions and deposition (Sect. 3.1), reflecting the added complexity of lake-specific characteristics and ecological factors. For example, the modeled decline in fish MeHg for lakes in Michigan's Upper Peninsula (UP) is moderate (0.25 % yr^{-1}). However, two virtual experiments reported by Perlinger et al. (2018) separate the effects of scenario-based atmospheric deposition and watershed sensitivity on fish MeHg responses (Ellipse A; symbol ∇). Applying Adirondack deposition to the Michigan UP lake resulted in increased modeled fish MeHg, whereas applying Adirondack watershed characteristics under the same deposition conditions led to a decrease, highlighting the influence of watershed properties. Similarly, under the high deposition reduction scenario involving a 50 % decrease in Hg

deposition (Ellipse B; symbol Δ), five integrated data points show substantial variability in fish MeHg responses under the same policy scenario (Knightes et al., 2009). Lakes with large surface areas, indicating greater direct atmospheric exposure, together with large watersheds and higher wetland percentages (e.g., bay lakes and coastal rivers) showed the greatest declines in fish MeHg. Intermediate declines occurred in seepage and stratified drainage lakes, whereas systems with lower wetland influence and weaker watershed-mediated Hg inputs (e.g., farm ponds) exhibited slower declines in fish MeHg (Knightes et al., 2009). Together, these findings highlight that while deposition strongly governs fish MeHg, lake characteristics can result in site-specific variability, which we elaborate further in Sect. 3.3.

Apart from the lake-specific characteristics, additional ecological and climate-related factors can modulate fish MeHg levels. These have been evident through many individual studies. In particular, the changes in fish MeHg concentrations documented at various lakes in Michigan's Upper Peninsula (UP), U.S. provides a key case study. Comparisons between modeled and observed changes in lake trout MeHg reveal notable discrepancies across different time periods.

Model simulations for lakes in Michigan's UP estimated modest annual fish MeHg declines ($-0.25\,\%\,yr^{-1}$ to $-1.48\,\%\,yr^{-1}$) during 2006–2050 under policy scenarios (Perlinger et al., 2018), whereas, observed lake trout data from lakes in Michigan's UP showed a sharper decline of $3.9\,\%\,yr^{-1}$ (2004–2015) (Zhou et al., 2017). The reduction was largely driven by a steep drop in fish MeHg before 2008 ($-11.7\,\%\,yr^{-1}$), followed by a subsequent plateau, which was attributed to climate-relevant changes in food web structure and amount of wet Hg deposition (Zhou et al., 2017). More recent work by (Lepak et al., 2025) also reported counterintuitive increases in fish MeHg despite declining local-regional Hg emissions and atmospheric deposition, attributing them to invasive dreissenid mussels that redirected trout toward lower-calorie, benthic prey, coupled with reduced lake productivity and slower fish growth. Stable isotope analyses of Hg (Δ^{199}Hg), together with carbon and nitrogen isotopes (δ^{13}C, δ^{15}N), confirmed these dietary and energy-flow changes (Lepak et al., 2019; 2025). Similarly, (Kerfoot et al., 2018) observed rising fish MeHg (1 %–3 $\%\,yr^{-1}$, 2001–2013) despite an 81 % regional emission decline, driven by wetland recovery and renewed methylation of legacy Hg.

Despite these ecological complexities, isotopic evidence provides further insight into system responsiveness. Stable-isotope evidence from the Great Lakes indicates that fish Hg isotopic signatures respond more rapidly to changes in atmospheric Hg concentrations than sedimentary records, suggesting that fish act as sensitive biosentinels of recent deposition trends (Lepak et al., 2025). Long-term whole-ecosystem isotope-labeled experiments in a boreal lake support this view, showing that reducing direct atmospheric inputs drives rapid declines in fish MeHg through food webs, even if watershed Hg is retained and mobilized more slowly (Blanchfield et al., 2022). Yet interacting stressors, such as invasive species, climate change, and enhanced wetland inflows, can amplify methylation and delay Hg recovery (Hall et al., 2023; Thompson et al., 2023; Rodríguez, 2023; McCarter et al., 2024; Lepak et al., 2025; Olson et al., 2025).

Collectively, these findings highlight the constraints of assuming that fish MeHg levels will decline in direct proportion to atmospheric deposition. They raise an important question for future assessments: do lake ecosystems truly follow linear dynamics, or do current models oversimplify the complex ecological, biogeochemical, and climate-driven interactions that regulate Hg uptake and bioaccumulation in natural ecosystems?

3.3 Influence of lake characteristics on projected fish MeHg responses

This section examines how lake-specific characteristics are represented across models when simulating future fish MeHg levels. To evaluate how these characteristics are treated within the model-simulated framework, we incorporated key environmental predictors used in the same studies analyzed in Sect. 3.2. These include lake area, watershed area, wetland percentage, and average depth, together with scenario-specific changes in Hg deposition as well as the corresponding changes in fish MeHg, into our statistical analyses (Knightes et al., 2009; Vijayaraghavan et al., 2014; Angot et al., 2018; Perlinger et al., 2018). The full list of used variables is provided in Table S4. Extensive empirical work has shown that fish MeHg levels respond to lake morphometry (area, depth, wetland extent) (Bodaly et al., 1993; Choy et al., 2009; Ackerman et al., 2019; Knott et al., 2020), watershed size and composition (Sonesten, 2003; Evans et al., 2005; Rypel, 2010; Marusczak et al., 2011; Eagles-Smith et al., 2016; Backstrom et al., 2020), water chemistry (pH, hardness, alkalinity) (McMurtry et al., 1989; Backstrom et al., 2020), hydrologic conditions (drainage pattern) (Grieb et al., 1990), geographical gradient (Morel et al., 1998), seasonal variability (Barletta et al., 2012; Keva et al., 2017; Mills et al., 2018), and fish-specific traits (age, size, trophic level) (Cizdziel et al., 2002; Evans et al., 2005; Marusczak et al., 2011; Backstrom et al., 2020). Together, these studies illustrate that multiple environmental processes regulate MeHg bioaccumulation, providing a basis for examining how Hg bioaccumulation models prioritize these same factors.

We first evaluated whether lake characteristics alone could explain variability in projected changes in fish MeHg across models using MLRM. No strong relationships were identified (Table S5). When scenario-specific changes in Hg deposition were incorporated, as described in Sect. 3.2, only deposition change ($p = 0.007$) and lake area ($p = 0.04$) emerged as significant predictors, while other variables contributed weakly (Table S6). These results motivated subsequent PCA analyses to examine how deposition and lake characteristics

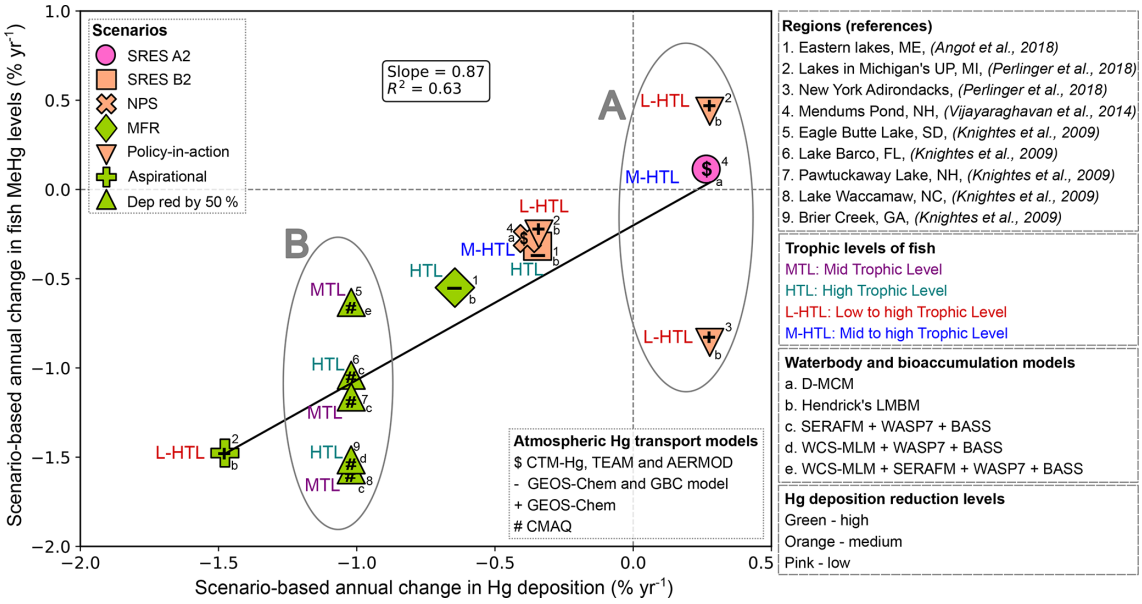

Figure 3. Relationship between scenario-based projected annual changes in atmospheric Hg deposition (% yr^{-1}) and corresponding changes in fish MeHg concentrations (% yr^{-1}) by 2050. Marker shapes (top left panel) denote Hg deposition scenarios, while special characters (bottom right panel) represent atmospheric Hg deposition models. Numbers shown in the top right panel correspond to study regions and references. Fish trophic levels are color-coded in the lower panel, and the bottom right panel also indicates waterbody and watershed type together with the bioaccumulation models used. Marker fill colors indicate the magnitude of Hg deposition reduction, classified as high (green), medium (orange), and low (pink).

interact collectively within Hg bioaccumulation model simulations.

PCA was conducted within a scenario-based modeling framework consistent with Sect. 3.2, using lake area, watershed area, wetland percentage, average depth, and projected changes in Hg deposition as explanatory variables, with projected changes in fish MeHg included as a supplementary variable. The resulting biplot (Fig. 4) summarizes dominant patterns of covariation, with the first two principal components explaining 70.82 % of the total variance (PC1 = 38.13 %, PC2 = 32.69 %). PC1 was primarily defined by lake area and wetland percentage, whereas PC2 was driven by average depth and Hg deposition change, with a moderate contribution from watershed area. Consistent with this structure, a MLRM using PC1 and PC2 explained a substantial portion of the variability in the simulated response variable (Change in fish MeHg) and was statistically significant ($R^2 = 0.57$; $F = 6.74$, $p = 0.01$). PC1 exhibited a significant negative association ($\beta = -0.26$, $p = 0.02$), indicating that systems with larger lake area and higher wetland coverage tend to show greater declines in fish MeHg in the model simulations. In contrast, PC2 showed a significant positive relationship ($\beta = 0.24$, $p = 0.04$). This component reflects a trade-off between atmospheric Hg loading and lake depth versus watershed influence (Fig. 4), such that the bioaccumulation models predict the greatest simulated MeHg increases (or smallest reductions) in deep, atmospherically impacted systems with relatively small contributing catchments. The proximity of the fish MeHg vector in Fig. 4 confirms that modeled future fish MeHg responses are structured along gradients of lake morphometry and atmospheric Hg loading.

Collectively, results from the MLRM and PCA analyses indicate that, within the modeling framework, scenario-specific changes in atmospheric Hg deposition consistently emerge as the dominant predictor of future fish MeHg responses, with lake area exerting a secondary influence, while wetland extent, average depth, and watershed area contributing primarily through multivariate structure in the PCA. Across these statistical approaches, deposition change explains the largest share of variance in modeled fish MeHg, reinforcing the central role of Hg-emission policies in shaping projected bioaccumulation outcomes in the model-simulated world. This finding mirrors the pattern of whole-ecosystem experimental studies showing declines in fish MeHg following reductions in Hg deposition (Blanchfield et al., 2022). However, comparisons between modeled projections and long-term observational records reveal a more complex reality. Case studies from lakes in Michigan's UP demonstrate that fish MeHg concentrations may increase, decrease, or respond nonlinearly despite substantial declines in atmospheric Hg deposition, reflecting the influence of ecological and biogeochemical processes not fully resolved by current models. These include food-web restructuring, invasive species, productivity shifts, wetland-mediated methylation, internal Hg cycling, and climate-driven changes in hydrology and redox conditions. Moreover, the negative association between

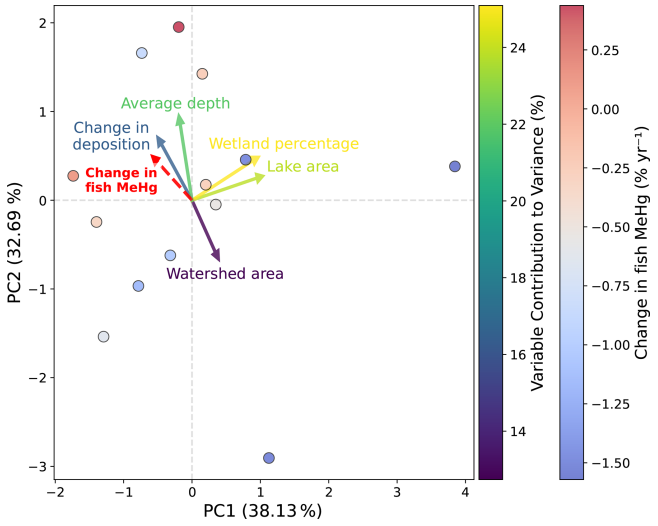

Figure 4. PCA biplot of environmental predictors and scenario-based Hg deposition. Points represent individual model realizations positioned by their PC1 and PC2 scores and colored by projected change in fish MeHg (% yr^{-1}). Solid arrows show predictor loadings (length and color indicate contribution to variance), and the dashed red arrow represents the supplementary projection of fish MeHg.

wetland extent and projected fish MeHg observed here in the PCA differs from many field studies, which commonly report elevated fish MeHg with increasing wetland coverage, although the magnitude and direction of this relationship vary with sulfate availability, dissolved organic matter, and hydrologic setting (Watras et al., 2005; Ackerman et al., 2019; Poulin et al., 2025). This apparent discrepancy likely reflects model assumptions regarding Hg loading pathways and response kinetics. Modeling frameworks derived from or conceptually similar to SERAFM assume relatively direct transfer of atmospherically deposited Hg from the catchment to the lake, with limited representation of hydrologic retention and delayed release from soils and wetlands (Perlinger et al., 2018). Under this structure, wetlands and large watersheds act as highly sensitive receptors of atmospheric Hg inputs, strengthening atmospheric–catchment coupling in wetland-dominated systems. Our supplemental regression analysis supports this interpretation, showing that watershed and wetland area are strong predictors of total Hg loading to the lake ($R^2 = 0.90$ and 0.87, respectively; $p < 0.0001$). In addition, PCA results indicate that lake morphometry controls model sensitivity, with large, shallow lakes responding strongly to deposition changes due to limited dilution. Fish MeHg concentrations are commonly estimated using a steady-state BAF approach, which does not capture the biological and ecological lag times required for fish populations to fully adjust to changes in water-column Hg exposure (Angot et al., 2018). Consequently, declines in modeled water-column Hg are translated into relatively rapid declines in fish MeHg, whereas in natural systems, Hg stored in wetland soils and catchment reservoirs can delay responses to emission reductions. Thus, although wetland-dominated systems often support higher absolute MeHg concentrations in empirical studies, they emerge in these simulations as the most dynamic responders to declining atmospheric inputs because legacy storage and delayed ecosystem adjustment are only partially represented. In contrast, emerging 3-D marine Hg models such as MERCY and OGSTM–BFM–Hg demonstrate how embedding Hg cycling and bioaccumulation in high-resolution physical–biogeochemical frameworks with multi-trophic food webs can resolve climate impacts and food-web–mediated exposure with far greater realism (Rosati et al., 2022; Bieser et al., 2023). Biogeochemical reaction rates and lake-chemistry variables (e.g., DOC, alkalinity, sulfur) could not be evaluated here due to data limitations but incorporating them in future work will be essential for linking model behavior with real-world ecosystem responses.

4 Conclusions

In summary, despite substantial differences among atmospheric models in spatial resolution, emission inventories, meteorological drivers, and redox chemistry, and despite variability in bioaccumulation models and ecosystem complexity, our study shows that they consistently predict strong linear relationships between emissions, deposition, and fish MeHg. Within the model world, deposition change and lake morphometry emerge as dominant predictors of future fish MeHg responses. Yet comparisons with observations reveal important departures from these idealized trends along both links of the causal chain (emissions → deposition, and deposition → fish MeHg). In particular, Hg bioaccumulation models generally capture the direction of change under emission controls but underrepresent the ecological, biogeochemical, and regional heterogeneity that governs response rate and magnitude. Empirical evidence shows fish MeHg can respond nonlinearly, with lags or partial decoupling from declining deposition due to food-web restructuring, invasive species, wetland-mediated methylation, internal cycling, and climate-driven changes in productivity and hydrology. These findings underscore the need to pair global modeling with long-term atmospheric, deposition, and ecological measurements, and to improve representation of watershed processes, food-web dynamics, and climate feedbacks to more accurately predict the benefits of emission reductions under the Minamata Convention.

Thus, although current models are powerful and indispensable tools, their orderly linearity invites reflection: do we truly capture the intricate feedbacks of the real atmosphere and natural ecosystems? To strengthen future assessments and policy strategies, we should enhance model complexity by incorporating nonlinear processes and bridge gaps

with observations through prioritized field studies and long-term monitoring. By doing so, we can better validate projections, uncover unaccounted-for interactions, and ensure models evolve in step with the complexity of Hg cycling.

Code and data availability. Custom scripts used for statistical analyses are available from the corresponding author upon reasonable request. All data analysed in this study are available from the cited publications. Any compiled datasets are available from the corresponding author upon reasonable request.

Supplement. The supplement related to this article is available online at https://doi.org/10.5194/bg-23-3387-2026-supplement.

Author contributions. HG compiled and curated the data, conducted the analyses, and led the writing of the manuscript. HL cross-checked and validated the compiled data. JH provided critical feedback and contributed to manuscript revision. HA provided scientific feedback and suggestions that helped improve the manuscript. SYK supervised the study and contributed to conceptualization and manuscript revision. All authors reviewed and approved the final manuscript.

Competing interests. The contact author has declared that none of the authors has any competing interests.

Disclaimer. Publisher's note: Copernicus Publications remains neutral with regard to jurisdictional claims made in the text, published maps, institutional affiliations, or any other geographical representation in this paper. The authors bear the ultimate responsibility for providing appropriate place names. Views expressed in the text are those of the authors and do not necessarily reflect the views of the publisher.

Acknowledgements. Henna Gull gratefully acknowledges financial support from the Government of Korea Scholarship (GKS). The authors thank POSTECH and the Department of Environmental Science and Engineering (DESE) for institutional support, and the Environmental and Health Assessment Laboratory for providing the research infrastructure and facilities used in this study.

Financial support. This work was supported by the National Research Foundation of Korea (NRF) grant funded by the Korea government (MSIT) (grant no. RS-2025-02263830).

Review statement. This paper was edited by Jane Kirk and reviewed by David Amptmeijer and one anonymous referee.

References

Ackerman, J. T., Fleck, J. A., Eagles-Smith, C. A., Marvin-DiPasquale, M., Windham-Myers, L., Herzog, M. P., and McQuillen, H. L.: Wetland management strategy to reduce mercury in water and bioaccumulation in fish, Environ. Toxicol. Chem., 38, 2178–2196, https://doi.org/10.1002/etc.4535, 2019.

Ahonen, S. A., Hayden, B., Leppänen, J. J., and Kahilainen, K. K.: Climate and productivity affect total mercury concentration and bioaccumulation rate of fish along a spatial gradient of subarctic lakes, Sci. Total Environ., 637/638, 1586–1596, https://doi.org/10.1016/j.scitotenv.2018.04.436, 2018.

Al-Sulaiti, M. M., Soubra, L., and Al-Ghouti, M. A.: The causes and effects of mercury and methylmercury contamination in the marine environment: A review, Curr. Pollut. Rep., 8, 249–272, https://doi.org/10.1007/s40726-022-00226-7, 2022.

AMAP/UNEP: Technical Background Report for the Global Mercury Assessment 2013, Arctic Monitoring and Assessment Programme, Oslo, Norway/UNEP Chemicals Branch, Geneva, Switzerland, vi C 263 pp., ISBN 9788279710806, 2013.

AMAP/UN Environment: Technical Background Report for the Global Mercury Assessment 2018, Arctic Monitoring and Assessment Programme, Oslo, Norway/UN Environment Programme, Chemicals and Health Branch, Geneva, Switzerland, viiiC426 pp., ISBN 9788279711087, 2019.

Angot, H., Hoffman, N., Giang, A., Thackray, C. P., Hendricks, A. N., Urban, N. R., and Selin, N. E.: Global and local impacts of delayed mercury mitigation efforts, Environ. Sci. Technol., 52, 12968–12977, https://doi.org/10.1021/acs.est.8b04542, 2018.

Ariya, P. A., Amyot, M., Dastoor, A., Deeds, D., Feinberg, A., Kos, G., Poulain, A., Ryjkov, A., Semeniuk, K., Subir, M., and Toyota, K.: Mercury physicochemical and biogeochemical transformation in the atmosphere and at atmospheric interfaces: A review and future directions, Chem. Rev., 115, 3760–3802, https://doi.org/10.1021/cr500667e, 2015.

Backstrom, C. H., Buckman, K., Molden, E., and Chen, C. Y.: Mercury levels in freshwater fish: Estimating concentration with fish length to determine exposures through fish consumption, Arch. Environ. Contam. Toxicol., 78, 604–621, https://doi.org/10.1007/s00244-020-00717-y, 2020.

Bank, M. S.: The mercury science-policy interface: History, evolution and progress of the Minamata Convention, Sci. Total Environ., 722, 137832, https://doi.org/10.1016/j.scitotenv.2020.137832, 2020.

Barber, M. C.: Bioaccumulation and Aquatic System Simulator (BASS) User's Manual Version 2.2. EPA Report No. 600/R-01/035, update 2.2, March 2008, 2008.

Barber, M. C.: Bioaccumulation and Aquatic System Simulator (BASS) User's Manual Version 2.3. EPA Report No. 600/R-01/035, update 2.3, October 2018, 2018.

Barletta, M., Lucena, L. R. R., Costa, M. F., Barbosa-Cintra, S. C. T., and Cysneiros, F. J. A.: The interaction rainfall vs. weight as determinant of total mercury concentration in fish from a tropical estuary, Environ. Pollut., 167, 1–6, https://doi.org/10.1016/j.envpol.2012.03.033, 2012.

Basu, N., Bastiansz, A., Dórea, J. G., Fujimura, M., Horvat, M., Shroff, E., Weihe, P., and Zastenskaya, I.: Our evolved understanding of the human health risks of mercury, Ambio, 52, 877–896, https://doi.org/10.1007/s13280-023-01831-6, 2023.

Bieser, J., Amptmeijer, D. J., Daewel, U., Kuss, J., Soerensen, A. L., and Schrum, C.: The 3D biogeochemical marine mercury cycling model MERCY v2.0 – linking atmospheric Hg to methylmercury in fish, Geosci. Model Dev., 16, 2649–2688, https://doi.org/10.5194/gmd-16-2649-2023, 2023.

Blanchfield, P. J., Rudd, J. W. M., Hrenchuk, L. E., Amyot, M., Babiarz, C. L., Beaty, K. G., Bodaly, R. A. D., Branfireun, B. A., Gilmour, C. C., Graydon, J. A., Hall, B. D., Harris, R. C., Heyes, A., Hintelmann, H., Hurley, J. P., Kelly, C. A., Krabbenhoft, D. P., Lindberg, S. E., Mason, R. P., Paterson, M. J., Podemski, C. L., Sandilands, K. A., Southworth, G. R., St. Louis, V. L., Tate, L. S., and Tate, M. T.: Experimental evidence for recovery of mercury-contaminated fish populations, Nature, 601, 74–78, https://doi.org/10.1038/s41586-021-04222-7, 2022.

Bodaly, R. A., Rudd, J. W. M., Fudge, R. J. P., and Kelly, C. A.: Mercury concentrations in fish related to size of remote Canadian Shield lakes, Can. J. Fish. Aquat. Sci., 50, 980–987, https://doi.org/10.1139/f93-113, 1993.

Bradford, M. A., Mallory, M. L., and O'Driscoll, N. J.: The complex interactions between sediment geochemistry, methylmercury production, and bioaccumulation in intertidal estuarine ecosystems: A focused review, Bull. Environ. Contam. Toxicol., 110, 26, https://doi.org/10.1007/s00128-022-03653-w, 2023.

Brocza, F. M., Rafaj, P., Sander, R., Wagner, F., and Jones, J. M.: Global scenarios of anthropogenic mercury emissions, Atmos. Chem. Phys., 24, 7385–7404, https://doi.org/10.5194/acp-24-7385-2024, 2024.

Bullock Jr., O. R., Atkinson, D., Braverman, T., Civerolo, K., Dastoor, A., Davignon, D., Ku, J., Lohman, K., Myers, T. C., Park, R. J., Seigneur, C., Selin, N. E., Sistla, G., and Vijayaraghavan, K.: An analysis of simulated wet deposition of mercury from the North American Mercury Model Intercomparison Study, J. Geophys. Res.-Atmos., 114, D08301, https://doi.org/10.1029/2008JD011224, 2009.

Burke, S. M., Muir, D. C. G., Kirk, J., Barst, B., Iqaluk, D., Wang, X., Pope, M., Lamoureux, S. F., and Lafrenière, M. J.: Divergent temporal trends of mercury in Arctic char from paired lakes influenced by climate-related drivers, Environ. Toxicol. Chem., 42, 2712–2725, https://doi.org/10.1002/etc.5744, 2023.

Capo, E., Cosio, C., Gascón Díez, E., Loizeau, J.-L., Mendes, E., Adatte, T., Franzenburg, S., and Bravo, A. G.: Anaerobic mercury methylators inhabit sinking particles of oxic water columns, Water Res., 229, 119368, https://doi.org/10.1016/j.watres.2022.119368, 2023.

Chen, L., Zhang, W., Zhang, Y., Tong, Y., Liu, M., Wang, H., Xie, H., and Wang, X.: Historical and future trends in global source-receptor relationships of mercury, Sci. Total Environ., 610/611, 24–31, https://doi.org/10.1016/j.scitotenv.2017.07.182, 2018.

Chen, X., Zhou, Y., Mai, Z., Cheng, H., and Wang, X.: Mangroves increased the mercury methylation potential in the sediment by producing organic matters and altering microbial methylators community, Sci. Total Environ., 962, 178457, https://doi.org/10.1016/j.scitotenv.2025.178457, 2025.

Choy, C. A., Popp, B. N., Kaneko, J. J., and Drazen, J. C.: The influence of depth on mercury levels in pelagic fishes and their prey, P. Natl. Acad. Sci. USA, 106, 13865–13869, https://doi.org/10.1073/pnas.0900711106, 2009.

Cizdziel, J. V., Hinners, T. A., Pollard, J. E., Heithmar, E. M., and Cross, C. L.: Mercury concentrations in fish from Lake Mead, USA, related to fish size, condition, trophic level, location, and consumption risk, Arch. Environ. Contam. Toxicol., 43, 309–317, https://doi.org/10.1007/s00244-002-1191-6, 2002.

Cohen, M. D., Draxler, R. R., Artz, R. S., Blanchard, P., Gustin, M. S., Han, Y.-J., Holsen, T. M., Jaffe, D. A., Kelley, P., Lei, H., Loughner, C. P., Luke, W. T., Lyman, S. N., Niemi, D., Pacyna, J. M., Pilote, M., Poissant, L., Ratte, D., Ren, X., Steenhuisen, F., Steffen, A., Tordon, R., and Wilson, S. J.: Modeling the global atmospheric transport and deposition of mercury to the Great Lakes, Elementa, 4, 000118, https://doi.org/10.12952/journal.elementa.000118, 2016.

Corbitt, E. S., Jacob, D. J., Holmes, C. D., Streets, D. G., and Sunderland, E. M.: Global source–receptor relationships for mercury deposition under present-day and 2050 emissions scenarios, Environ. Sci. Technol., 45, 10477–10484, https://doi.org/10.1021/es202496y, 2011.

Dai, S.-S., Yang, Z., Tong, Y., Chen, L., Liu, S.-Y., Pan, R., Li, Y., Zhang, C.-J., Liu, Y.-R., and Huang, Q.: Global distribution and environmental drivers of methylmercury production in sediments, J. Hazard. Mater., 407, 124700, https://doi.org/10.1016/j.jhazmat.2020.124700, 2021.

De Simone, F., Artaxo, P., Bencardino, M., Cinnirella, S., Carbone, F., D'Amore, F., Dommergue, A., Feng, X. B., Gencarelli, C. N., Hedgecock, I. M., Landis, M. S., Sprovieri, F., Suzuki, N., Wängberg, I., and Pirrone, N.: Particulate-phase mercury emissions from biomass burning and impact on resulting deposition: A modelling assessment, Atmos. Chem. Phys., 17, 1881–1899, https://doi.org/10.5194/acp-17-1881-2017, 2017.

Dibble, T. S., Zelie, M. J., and Mao, H.: Thermodynamics of reactions of ClHg and BrHg radicals with atmospherically abundant free radicals, Atmos. Chem. Phys., 12, 10271–10279, https://doi.org/10.5194/acp-12-10271-2012, 2012.

Eagles-Smith, C. A., Ackerman, J. T., Willacker, J. J., Tate, M. T., Lutz, M. A., Fleck, J. A., Stewart, A. R., Wiener, J. G., Evers, D. C., Lepak, J. M., Davis, J. A., and Pritz, C. F.: Spatial and temporal patterns of mercury concentrations in freshwater fish across the Western United States and Canada, Sci. Total Environ., 568, 1171–1184, https://doi.org/10.1016/j.scitotenv.2016.03.229, 2016.

Emmerton, C. A., Drevnick, P. E., Serbu, J. A., Cooke, C. A., Graydon, J., Reichert, M., Evans, M., and McMaster, M.: Downstream modification of mercury in diverse river systems underscores the role of local conditions in fish bioaccumulation, Ecosystems, 26, 114–133, https://doi.org/10.1007/s10021-022-00745-w, 2023.

Engstrom, D. R., Fitzgerald, W. F., Cooke, C. A., Lamborg, C. H., Drevnick, P. E., Swain, E. B., Balogh, S. J., and Balcom, P. H.: Atmospheric Hg emissions from preindustrial gold and silver extraction in the Americas: A reevaluation from lake-sediment archives, Environ. Sci. Technol., 48, 6533–6543, https://doi.org/10.1021/es405558e, 2014.

Evans, M. S., Lockhart, W. L., Doetzel, L., Low, G., Muir, D., Kidd, K., Stephens, G., and Delaronde, J.: Elevated mercury concentrations in fish in lakes in the Mackenzie River Basin: The role of physical, chemical, and biological factors, Sci. Total Environ., 351/352, 479–500, https://doi.org/10.1016/j.scitotenv.2004.12.086, 2005.

Feng, X., Fu, X., Zhang, H., Wang, X., Jia, L., Zhang, L., Lin, C.-J., Huang, J.-H., Liu, K., and Wang, S.: Combating air pollution sig-

nificantly reduced air mercury concentrations in China, Natl. Sci. Rev., 11, nwae264, https://doi.org/10.1093/nsr/nwae264, 2024.

Geyman, B. M., Streets, D. G., Thackray, C. P., Olson, C. L., Schaefer, K., and Sunderland, E. M.: Projecting global mercury emissions and deposition under the Shared Socioeconomic Pathways, Earth's Future, 12, e2023EF004231, https://doi.org/10.1029/2023EF004231, 2024.

Geyman, B. M., Streets, D. G., Olson, C. I., Thackray, C. P., Olson, C. L., Schaefer, K., Krabbenhoft, D. P., and Sunderland, E. M.: Cumulative anthropogenic impacts of past and future emissions and releases on the global mercury cycle, Environ. Sci. Technol., 59, 8578–8590, https://doi.org/10.1021/acs.est.4c13434, 2025.

Giang, A. and Selin, N. E.: Benefits of mercury controls for the United States, P. Natl. Acad. Sci. USA, 113, 286–291, https://doi.org/10.1073/pnas.1514395113, 2016.

Giang, A., Stokes, L. C., Streets, D. G., Corbitt, E. S., and Selin, N. E.: Impacts of the Minamata Convention on mercury emissions and global deposition from coal-fired power generation in Asia, Environ. Sci. Technol., 49, 5326–5335, https://doi.org/10.1021/acs.est.5b00074, 2015.

Gidley, P. T., Kreitinger, J. P., Zakikhani, M., and Suedel, B. C.: Methylmercury screening models for surface water habitat restoration: a case study in Duluth-Superior Harbor, Environmental Laboratory (U.S.), https://doi.org/10.21079/11681/25606, 2017.

Gillies, E. J., Li, M.-L., Christensen, V., Hoover, C., Sora, K. J., Loseto, L. L., Cheung, W. W. L., Angot, H., and Giang, A.: Exploring drivers of historic mercury trends in beluga whales using an ecosystem modeling approach, ACS Environ. Au., 4, 219–235, https://doi.org/10.1021/acsenvironau.3c00072, 2024.

Gilmour, C. C., Podar, M., Bullock, A. L., Graham, A. M., Brown, S. D., Somenahally, A. C., Johs, A., Hurt Jr., R. A., Bailey, K. L., and Elias, D. A.: Mercury methylation by novel microorganisms from new environments, Environ. Sci. Technol., 47, 11810–11820, https://doi.org/10.1021/es403075t, 2013.

Greenfield, J., Dai, T., and Manguerra, H. B.: Watershed modeling extensions of the Watershed Characterization System, 1615–1628, https://www.accesswater.org/publications/proceedings/-289221/watershed-modeling-extensions-of-the-watershed-characterization-system (last access: 30 April 2022), 2002.

Grieb, T. M., Bowie, G. L., Driscoll, C. T., Gloss, S. P., Schofield, C. L., and Porcella, D. B.: Factors affecting mercury accumulation in fish in the Upper Michigan Peninsula, Environ. Toxicol. Chem., 9, 919–930, https://doi.org/10.1002/etc.5620090710, 1990.

Guerrero, S. and Schneider, L.: The global roots of pre-1900 legacy mercury, P. Natl. Acad. Sci. USA, 120, e2304059120, https://doi.org/10.1073/pnas.2304059120, 2023.

Gustin, M. S., Lindberg, S. E., and Weisberg, P. J.: An update on the natural sources and sinks of atmospheric mercury, Appl. Geochem., 23, 482–493, https://doi.org/10.1016/j.apgeochem.2007.12.010, 2008.

Gworek, B., Dmuchowski, W., and Baczewska-Dąbrowska, A. H.: Mercury in the terrestrial environment: A review, Environ. Sci. Eur., 32, 128, https://doi.org/10.1186/s12302-020-00401-x, 2020.

Hall, B. D., Liu, S., Hoggarth, C. G. J., Bates, L. M., Boczulak, S. A., Schmidt, J. D., and Ireson, A. M.: Wet–dry cycles influence methylmercury concentrations in water in seasonal prairie wetland ponds, FACETS, 8, 1–14, https://doi.org/10.1139/facets-2022-0168, 2023.

Harris, R. C. and Bodaly, R. A.: Temperature, growth and dietary effects on fish mercury dynamics in two Ontario lakes, Biogeochemistry, 40, 175–187, https://doi.org/10.1023/A:1005986505407, 1998.

Harris, R. C., Rudd, J. W. M., Amyot, M., Babiarz, C. L., Beaty, K. G., Blanchfield, P. J., Bodaly, R. A., Branfireun, B. A., Gilmour, C. C., Graydon, J. A., Heyes, A., Hintelmann, H., Hurley, J. P., Kelly, C. A., Krabbenhoft, D. P., Lindberg, S. E., Mason, R. P., Paterson, M. J., Podemski, C. L., Robinson, A., Sandilands, K. A., Southworth, G. R., St. Louis, V. L., and Tate, M. T.: Whole-ecosystem study shows rapid fish-mercury response to changes in mercury deposition, P. Natl. Acad. Sci. USA, 104, 16586–16591, https://doi.org/10.1073/pnas.0704186104, 2007.

Hendricks, A.: A model to predict concentrations and uncertainty for mercury species in lakes, MSc thesis, Michigan Technological University, https://doi.org/10.37099/mtu.dc.etdr/585, 2018.

Holloway, T., Voigt, C., Morton, J., Spak, S. N., Rutter, A. P., and Schauer, J. J.: An assessment of atmospheric mercury in the Community Multiscale Air Quality (CMAQ) model at an urban site and a rural site in the Great Lakes Region of North America, Atmos. Chem. Phys., 12, 7117–7133, https://doi.org/10.5194/acp-12-7117-2012, 2012.

Holmes, C. D., Jacob, D. J., Corbitt, E. S., Mao, J., Yang, X., Talbot, R., and Slemr, F.: Global atmospheric model for mercury including oxidation by bromine atoms, Atmos. Chem. Phys., 10, 12037–12057, https://doi.org/10.5194/acp-10-12037-2010, 2010.

Horowitz, H. M., Jacob, D. J., Zhang, Y., Dibble, T. S., Slemr, F., Amos, H. M., Schmidt, J. A., Corbitt, E. S., Marais, E. A., and Sunderland, E. M.: A new mechanism for atmospheric mercury redox chemistry: Implications for the global mercury budget, Atmos. Chem. Phys., 17, 6353–6371, https://doi.org/10.5194/acp-17-6353-2017, 2017.

Kerfoot, W. C., Urban, N. R., McDonald, C. P., Zhang, H., Rossmann, R., Perlinger, J. A., Khan, T., Hendricks, A., Priyadarshini, M., and Bolstad, M.: Mining legacy across a wetland landscape: High mercury in Upper Peninsula (Michigan) rivers, lakes, and fish, Environ. Sci.-Process. Impact., 20, 708–733, https://doi.org/10.1039/C7EM00521K, 2018.

Keva, O., Hayden, B., Harrod, C., and Kahilainen, K. K.: Total mercury concentrations in liver and muscle of European whitefish (Coregonus lavaretus (L.)) in a subarctic lake – assessing the factors driving year-round variation, Environ. Pollut., 231, 1518–1528, https://doi.org/10.1016/j.envpol.2017.09.012, 2017.

Kidd, K. A., Muir, D. C. G., Evans, M. S., Wang, X., Whittle, M., Swanson, H. K., and Guildford, S. J.: Biomagnification of mercury through lake trout (Salvelinus namaycush) food webs of lakes with different physical, chemical and biological characteristics, Sci. Total Environ., 438, 135–143, https://doi.org/10.1016/j.scitotenv.2012.08.057, 2012.

Kim, M.-K. and Zoh, K.-D.: Fate and transport of mercury in environmental media and human exposure, J. Prev. Med. Public Health, 45, 335–343, https://doi.org/10.3961/jpmph.2012.45.6.335, 2012.

Knightes, C. D.: Development and test application of a screening-level mercury fate model and tool for evaluating wildlife ex-

posure risk for surface waters with mercury-contaminated sediments (SERAFM), Environ. Modell. Softw., 23, 495–510, https://doi.org/10.1016/j.envsoft.2007.07.002, 2008.

Knightes, C. D., Sunderland, E. M., Barber, M. C., Johnston, J. M., and Ambrose, R. B.: Application of ecosystem-scale fate and bioaccumulation models to predict fish mercury response times to changes in atmospheric deposition, Environ. Toxicol. Chem., 28, 881–893, https://doi.org/10.1897/08-242R.1, 2009.

Knott, K. K., O'Hearn, R., Niswonger, D., Lawson, L., North, R., Obrecht, D., Tracy-Smith, E., Voss, R., Wenzel, J., and McKee, M.: Physical, chemical, and biological factors that contribute to the variability of mercury concentrations in largemouth bass Micropterus salmoides from Missouri reservoirs, Arch. Environ. Contam. Toxicol., 78, 284–293, https://doi.org/10.1007/s00244-019-00697-8, 2020.

Kumar, A. and Wu, S.: Mercury pollution in the Arctic from wildfires: Source attribution for the 2000s, Environ. Sci. Technol., 53, 11269–11275, https://doi.org/10.1021/acs.est.9b01773, 2019.

Kumar, A., Wu, S., Huang, Y., Liao, H., and Kaplan, J. O.: Mercury from wildfires: Global emission inventories and sensitivity to 2000–2050 global change, Atmos. Environ., 173, 6–15, https://doi.org/10.1016/j.atmosenv.2017.10.061, 2018.

Lei, H., Wuebbles, D. J., Liang, X.-Z., Tao, Z., Olsen, S., Artz, R., Ren, X., and Cohen, M.: Projections of atmospheric mercury levels and their effect on air quality in the United States, Atmos. Chem. Phys., 14, 783–795, https://doi.org/10.5194/acp-14-783-2014, 2014.

Leiva González, J., Diaz-Robles, L. A., Cereceda-Balic, F., Pino-Cortés, E., and Campos, V.: Atmospheric modelling of mercury in the Southern Hemisphere and future research needs: A review, Atmosphere, 13, 1226, https://doi.org/10.3390/atmos13081226, 2022.

Lepak, R. F., Hoffman, J. C., Janssen, S. E., Krabbenhoft, D. P., Ogorek, J. M., DeWild, J. F., Tate, M. T., Babiarz, C. L., Yin, R., Murphy, E. W., Engstrom, D. R., and Hurley, J. P.: Mercury source changes and food web shifts alter contamination signatures of predatory fish from Lake Michigan, P. Natl. Acad. Sci. USA, 116, 23600–23608, https://doi.org/10.1073/pnas.1907484116, 2019.

Lepak, R. F., Hoffman, J. C., Janssen, S. E., Tate, M. T., Shanoff, M. B., Mahon, M. B., Rumschlag, S. L., Yarnes, C. T., Lenell, B. A., Krabbenhoft, D. P., Ogorek, J. M., and Hurley, J. P.: Ecological factors decouple Great Lakes fish mercury concentrations trends from decadal declines in atmospheric mercury, Environ. Sci. Technol., 59, 11799–11808, https://doi.org/10.1021/acs.est.5c01359, 2025.

Li, C., Sonke, J. E., Le Roux, G., Piotrowska, N., Van der Putten, N., Roberts, S. J., Daley, T., Rice, E., Gehrels, R., Hodgson, D. A., and De Vleeschouwer, F.: Unequal anthropogenic enrichment of mercury in Earth's Northern and Southern Hemispheres, ACS Earth Space Chem., 4, 2073–2081, https://doi.org/10.1021/acsearthspacechem.0c00220, 2020.

Lindenschmidt, K.-E.: Testing for the transferability of a water quality model to areas of similar spatial and temporal scale based on an uncertainty vs. complexity hypothesis, Ecol. Complex., 3, 241–252, https://doi.org/10.1016/j.ecocom.2006.05.002, 2006.

Liu, K., Wu, Q., Wang, L., Wang, S., Liu, T., Ding, D., Tang, Y., Li, G., Tian, H., Duan, L., and Hao, J.: Measure-specific effectiveness of air pollution control on China's atmospheric mercury concentration and deposition during 2013–2017, Environ. Sci. Technol., 53, 8938–8946, https://doi.org/10.1021/acs.est.9b02428, 2019.

Liu, M., Mason, R. P., Vlahos, P., Whitney, M. M., Zhang, Q., Warren, J. K., Wang, X., and Baumann, Z.: Riverine discharge fuels the production of methylmercury in a large temperate estuary, Environ. Sci. Technol., 57, 13056–13066, https://doi.org/10.1021/acs.est.3c00473, 2023.

Marusczak, N., Larose, C., Dommergue, A., Paquet, S., Beaulne, J.-S., Maury-Brachet, R., Lucotte, M., Nedjai, R., and Ferrari, C. P.: Mercury and methylmercury concentrations in high altitude lakes and fish (Arctic charr) from the French Alps related to watershed characteristics, Sci. Total Environ., 409, 1909–1915, https://doi.org/10.1016/j.scitotenv.2011.02.015, 2011.

Massoudieh, A., Žagar, D., Green, P. G., Cabrera-Toledo, C., Horvat, M., Ginn, T. R., Barkouki, T., Weathers, T., and Bombardelli, F. A.: Modeling mercury fate and transport in aquatic systems, in: Advances in Environmental Fluid Mechanics, edited by: Mihailovic, D. T. and Gualtieri, C., World Scientific, 275–308, https://doi.org/10.1142/9789814293006_0013, 2010.

McCarter, C. P. R., Sebestyen, S. D., Jeremiason, J. D., Nater, E. A., and Kolka, R. K.: Methylmercury export from a headwater peatland catchment decreased with cleaner emissions despite opposing effect of climate warming, Water Resour. Res., 60, e2023WR036513, https://doi.org/10.1029/2023WR036513, 2024.

McMurtry, M. J., Wales, D. L., Scheider, W. A., Beggs, G. L., and Dimond, P. E.: Relationship of mercury concentrations in lake trout (Salvelinus namaycush) and smallmouth bass (Micropterus dolomieui) to the physical and chemical characteristics of Ontario lakes, Can. J. Fish. Aquat. Sci., 46, 426–434, https://doi.org/10.1139/f89-057, 1989.

Médieu, A., Point, D., Sonke, J. E., Angot, H., Allain, V., Bodin, N., Adams, D. H., Bignert, A., Streets, D. G., Buchanan, P. B., Heimbürger-Boavida, L.-E., Pethybridge, H., Gillikin, D. P., Ménard, F., Choy, C. A., Itai, T., Bustamante, P., Dhurmeea, Z., Ferriss, B. E., Bourlès, B., Habasque, J., Verheyden, A., Munaron, J.-M., Laffont, L., Gauthier, O., and Lorrain, A.: Stable tuna mercury concentrations since 1971 illustrate marine inertia and the need for strong emission reductions under the Minamata Convention, Environ. Sci. Technol. Lett., 11, 250–258, https://doi.org/10.1021/acs.estlett.3c00949, 2024.

Mills, N., Cashatt, D., Weber, M. J., and Pierce, C. L.: A case study and a meta-analysis of seasonal variation in fish mercury concentrations, Ecotoxicology, 27, 641–649, https://doi.org/10.1007/s10646-018-1942-4, 2018.

Moore, C. W., Obrist, D., and Luria, M.: Atmospheric mercury depletion events at the Dead Sea: Spatial and temporal aspects, Atmos. Environ., 69, 231–239, https://doi.org/10.1016/j.atmosenv.2012.12.020, 2013.

Morel, F. M. M., Kraepiel, A. M. L., and Amyot, M.: The chemical cycle and bioaccumulation of mercury, Annu. Rev. Ecol. Syst., 29, 543–566, https://doi.org/10.1146/annurev.ecolsys.29.1.543, 1998.

Nakicenovic, N., Alcamo, J., Grubler, A., Riahi, K., Roehrl, R. A., Rogner, H.-H., and Victor, N.: Special Report on Emissions Scenarios (SRES), A Special Report of Working Group III of the Intergovernmental Panel on Climate Change, Cambridge University Press, Cambridge, ISBN 0521804930, 2000.

Nriagu, J. O.: Legacy of mercury pollution, Nature, 363, 589, https://doi.org/10.1038/363589a0, 1993.

Nriagu, J. O.: Mercury pollution from the past mining of gold and silver in the Americas, Sci. Total Environ., 149, 167–181, https://doi.org/10.1016/0048-9697(94)90177-5, 1994.

Obrist, D., Kirk, J. L., Zhang, L., Sunderland, E. M., Jiskra, M., and Selin, N. E.: A review of global environmental mercury processes in response to human and natural perturbations: Changes of emissions, climate, and land use, Ambio, 47, 116–140, https://doi.org/10.1007/s13280-017-1004-9, 2018.

Ogorek, J. M., Lepak, R. F., Hoffman, J. C., DeWild, J. F., Rosera, T. J., Tate, M. T., Hurley, J. P., and Krabbenhoft, D. P.: Enhanced susceptibility of methylmercury bioaccumulation into seston of the Laurentian Great Lakes, Environ. Sci. Technol., 55, 12714–12723, https://doi.org/10.1021/acs.est.1c02319, 2021.

Olson, C. I., Jane, S. F., Geyman, B. M., Montesdeoca, M. R., McHale, P. J., Beier, C. M., Mills, J. S., McIntyre, P. B., Sunderland, E. M., and Driscoll, C. T.: Soil mercury accumulation delays fish recovery from atmospheric deposition declines, Environ. Sci. Technol., 59, 12656–12666, https://doi.org/10.1021/acs.est.5c00834, 2025.

Outridge, P. M., Mason, R. P., Wang, F., Guerrero, S., and Heimbürger-Boavida, L. E.: Updated global and oceanic mercury budgets for the United Nations Global Mercury Assessment 2018, Environ. Sci. Technol., 52, 11466–11477, https://doi.org/10.1021/acs.est.8b01246, 2018.

Pacyna, E. G., Pacyna, J. M., Steenhuisen, F., and Wilson, S.: Global anthropogenic mercury emission inventory for 2000, Atmos. Environ., 40, 4048–4063, https://doi.org/10.1016/j.atmosenv.2006.03.041, 2006.

Pacyna, J. M., Travnikov, O., De Simone, F., Hedgecock, I. M., Sundseth, K., Pacyna, E. G., Steenhuisen, F., Pirrone, N., Munthe, J., and Kindbom, K.: Current and future levels of mercury atmospheric pollution on a global scale, Atmos. Chem. Phys., 16, 12495–12511, https://doi.org/10.5194/acp-16-12495-2016, 2016.

Perlinger, J. A., Urban, N. R., Giang, A., Selin, N. E., Hendricks, A. N., Zhang, H., Kumar, A., Wu, S., Gagnon, V. S., Gorman, H. S., and Norman, E. S.: Responses of deposition and bioaccumulation in the Great Lakes region to policy and other large-scale drivers of mercury emissions, Environ. Sci.-Process. Impact., 20, 195–209, https://doi.org/10.1039/C7EM00547D, 2018.

Peterson, B. D., Janssen, S. E., Poulin, B. A., Ogorek, J. M., White, A., McDaniel, E. A., Marick, R. A., Armstrong, G. J., Scheel, N. D., Tate, M. T., Krabbenhoft, D. P., and McMahon, K. D.: Sulfate reduction drives elevated methylmercury formation in the water column of a eutrophic freshwater lake, Environ. Sci. Technol., 59, 6799–6811, https://doi.org/10.1021/acs.est.4c12759, 2025.

Pirrone, N., Cinnirella, S., Feng, X., Finkelman, R. B., Friedli, H. R., Leaner, J., Mason, R., Mukherjee, A. B., Stracher, G. B., Streets, D. G., and Telmer, K.: Global mercury emissions to the atmosphere from anthropogenic and natural sources, Atmos. Chem. Phys., 10, 5951–5964, https://doi.org/10.5194/acp-10-5951-2010, 2010.

Poulin, B. A., Tate, M. T., Janssen, S. E., Aiken, G. R., and Krabbenhoft, D. P.: A comprehensive sulfate and DOM framework to assess methylmercury formation and risk in subtropical wetlands, Nat. Commun., 16, 4253, https://doi.org/10.1038/s41467-025-59581-w, 2025.

Rafaj, P., Bertok, I., Cofala, J., and Schöpp, W.: Scenarios of global mercury emissions from anthropogenic sources, Atmos. Environ., 79, 472–479, https://doi.org/10.1016/j.atmosenv.2013.06.042, 2013.

Rodríguez, J.: Mercury methylation in boreal aquatic ecosystems under oxic conditions and climate change: A review, Front. Mar. Sci., 10, 1198263, https://doi.org/10.3389/fmars.2023.1198263, 2023.

Rosati, G., Canu, D., Lazzari, P., and Solidoro, C.: Assessing the spatial and temporal variability of methylmercury biogeochemistry and bioaccumulation in the Mediterranean Sea with a coupled 3D model, Biogeosciences, 19, 3663–3682, https://doi.org/10.5194/bg-19-3663-2022, 2022.

Russ, P., Ciscar, J. C., Saveyn, B., Soria, A., Szabo, L., Ierland, T.V., Regemorter, D.V., and Virdis, R.: Economic assessment of post-2012 global climate policies: analysis of greenhouse gas emission reduction scenarios with the POLES and GEM-E3 models, JRC Sci. Tech. Rep., JRC50307, European Commission, Luxembourg, https://doi.org/10.2791/70332, 2009.

Rypel, A. L.: Mercury concentrations in lentic fish populations related to ecosystem and watershed characteristics, Ambio, 39, 14–19, https://doi.org/10.1007/s13280-009-0001-z, 2010.

Schaefer, K., Elshorbany, Y., Jafarov, E., Schuster, P. F., Striegl, R. G., Wickland, K. P., and Sunderland, E. M.: Potential impacts of mercury released from thawing permafrost, Nat. Commun., 11, 4650, https://doi.org/10.1038/s41467-020-18398-5, 2020.

Schartup, A. T., Thackray, C. P., Qureshi, A., Dassuncao, C., Gillespie, K., Hanke, A., and Sunderland, E. M.: Climate change and overfishing increase neurotoxicant in marine predators, Nature, 572, 648–650, https://doi.org/10.1038/s41586-019-1468-9, 2019.

Schartup, A. T., Soerensen, A. L., Angot, H., Bowman, K., and Selin, N. E.: What are the likely changes in mercury concentration in the Arctic atmosphere and ocean under future emissions scenarios?, Sci. Total Environ., 836, 155477, https://doi.org/10.1016/j.scitotenv.2022.155477, 2022.

Selin, N. E.: Global biogeochemical cycling of mercury: A review, Annu. Rev. Environ. Resour., 34, 43–63, https://doi.org/10.1146/annurev.environ.051308.084314, 2009.

Selin, N. E. and Selin, H.: Global politics of mercury pollution: The need for multi-scale governance, Rev. Eur. Community Int. Environ. Law, 15, 258–269, https://doi.org/10.1111/j.1467-9388.2006.00529.x, 2006.

Shah, V., Jaeglé, L., Gratz, L. E., Ambrose, J. L., Jaffe, D. A., Selin, N. E., Song, S., Campos, T. L., Flocke, F. M., Reeves, M., Stechman, D., Stell, M., Festa, J., Stutz, J., Weinheimer, A. J., Knapp, D. J., Montzka, D. D., Tyndall, G. S., Apel, E. C., Hornbrook, R. S., Hills, A. J., Riemer, D. D., Blake, N. J., Cantrell, C. A., and Mauldin III, R. L.: Origin of oxidized mercury in the summertime free troposphere over the southeastern US, Atmos. Chem. Phys., 16, 1511–1530, https://doi.org/10.5194/acp-16-1511-2016, 2016.

Shah, V., Jacob, D. J., Thackray, C. P., Wang, X., Sunderland, E. M., Dibble, T. S., Saiz-Lopez, A., Černušák, I., Kellö, V., Castro, P. J., Wu, R., and Wang, C.: Improved mechanistic model of the atmospheric redox chemistry of mercury, Environ. Sci. Technol., 55, 14445–14456, https://doi.org/10.1021/acs.est.1c03160, 2021.

Sonesten, L.: Fish mercury levels in lakes–adjusting for Hg and fish-size covariation, Environ. Pollut., 125, 255–265, https://doi.org/10.1016/S0269-7491(03)00051-4, 2003.

Sonke, J. E., Angot, H., Zhang, Y., Poulain, A., Björn, E., and Schartup, A.: Global change effects on biogeochemical mercury cycling, Ambio, 52, 853–876, https://doi.org/10.1007/s13280-023-01855-y, 2023.

Streets, D. G., Zhang, Q., and Wu, Y.: Projections of global mercury emissions in 2050, Environ. Sci. Technol., 43, 2983–2988, https://doi.org/10.1021/es802474j, 2009.

Streets, D. G., Devane, M. K., Lu, Z., Bond, T. C., Sunderland, E. M., and Jacob, D. J.: All-time releases of mercury to the atmosphere from human activities, Environ. Sci. Technol., 45, 10485–10491, https://doi.org/10.1021/es202765m, 2011.

Streets, D. G., Horowitz, H. M., Jacob, D. J., Lu, Z., Levin, L., ter Schure, A. F. H., and Sunderland, E. M.: Total mercury released to the environment by human activities, Environ. Sci. Technol., 51, 5969–5977, https://doi.org/10.1021/acs.est.7b00451, 2017.

Streets, D. G., Horowitz, H. M., Lu, Z., Levin, L., Thackray, C. P., and Sunderland, E. M.: Five hundred years of anthropogenic mercury: Spatial and temporal release profiles, Environ. Res. Lett., 14, 084004, https://doi.org/10.1088/1748-9326/ab281f, 2019.

Sun, R., Yuan, J., Sonke, J. E., Zhang, Y., Zhang, T., Zheng, W., Chen, S., Meng, M., Chen, J., Liu, Y., Peng, X., and Liu, C.: Methylmercury produced in upper oceans accumulates in deep Mariana Trench fauna, Nat. Commun., 11, 3389, https://doi.org/10.1038/s41467-020-17045-3, 2020.

Sunderland, E. M. and Selin, N. E.: Future trends in environmental mercury concentrations: Implications for prevention strategies, Environ. Health, 12, 2, https://doi.org/10.1186/1476-069X-12-2, 2013.

Thompson, L. M., Low, M., Shewan, R., Schulze, C., Simba, M., Sonnentag, O., Tank, S. E., and Olefeldt, D.: Concentrations and yields of mercury, methylmercury, and dissolved organic carbon from contrasting catchments in the discontinuous permafrost region, western Canada, Water Resour. Res., 59, e2023WR034848, https://doi.org/10.1029/2023WR034848, 2023.

Travnikov, O., Angot, H., Artaxo, P., Bencardino, M., Bieser, J., D'Amore, F., Dastoor, A., De Simone, F., Diéguez, M. C., Dommergue, A., Ebinghaus, R., Feng, X. B., Gencarelli, C. N., Hedgecock, I. M., Magand, O., Martin, L., Matthias, V., Mashyanov, N., Pirrone, N., Ramachandran, R., Read, K. A., Ryjkov, A., Selin, N. E., Sena, F., Song, S., Sprovieri, F., Wip, D., Wängberg, I., and Yang, X.: Multi-model study of mercury dispersion in the atmosphere: Atmospheric processes and model evaluation, Atmos. Chem. Phys., 17, 5271–5295, https://doi.org/10.5194/acp-17-5271-2017, 2017.

Trudel, M. and Rasmussen, J. B.: Bioenergetics and mercury dynamics in fish: A modelling perspective, Can. J. Fish. Aquat. Sci., 63, 1890–1902, https://doi.org/10.1139/f06-081, 2006.

Vijayaraghavan, K., Levin, L., Parker, L., Yarwood, G., and Streets, D.: Response of fish tissue mercury in a freshwater lake to local, regional, and global changes in mercury emissions, Environ. Toxicol. Chem., 33, 1238–1247, https://doi.org/10.1002/etc.2584, 2014.

Vuksanovic, V., De Smedt, F., and Van Meerbeeck, S.: Transport of polychlorinated biphenyls (PCB) in the Scheldt Estuary simulated with the water quality model WASP, J. Hydrol., 174, 1–18, https://doi.org/10.1016/0022-1694(95)02759-9, 1996.

Wang, F., Outridge, P. M., Feng, X., Meng, B., Heimbürger-Boavida, L.-E., and Mason, R. P.: How closely do mercury trends in fish and other aquatic wildlife track those in the atmosphere? – Implications for evaluating the effectiveness of the Minamata Convention, Sci. Total Environ., 674, 58–70, https://doi.org/10.1016/j.scitotenv.2019.04.101, 2019.

Watras, C. J., Morrison, K. A., Kent, A., Price, N., Regnell, O., Eckley, C., Hintelmann, H., and Hubacher, T.: Sources of methylmercury to a wetland-dominated lake in northern Wisconsin, Environ. Sci. Technol., 39, 4747–4758, https://doi.org/10.1021/es040561g, 2005.

Willacker, J. J., Eagles-Smith, C. A., and Blazer, V. S.: Mercury bioaccumulation in freshwater fishes of the Chesapeake Bay watershed, Ecotoxicology, 29, 459–484, https://doi.org/10.1007/s10646-020-02193-5, 2020.

Wu, P., Dutkiewicz, S., Monier, E., and Zhang, Y.: Bottom-heavy trophic pyramids impair methylmercury biomagnification in the marine plankton ecosystems, Environ. Sci. Technol., 55, 15476–15483, https://doi.org/10.1021/acs.est.1c04083, 2021.

Xu, X., Feng, X., Lin, H., Zhang, P., Huang, S., Song, Z., Peng, Y., Fu, T.-M., and Zhang, Y.: Modeling the high-mercury wet deposition in the southeastern US with WRF-GC-Hg v1.0, Geosci. Model Dev., 15, 3845–3859, https://doi.org/10.5194/gmd-15-3845-2022, 2022.

Zhang, H., Wu, S., and Leibensperger, E. M.: Source-receptor relationships for atmospheric mercury deposition in the context of global change, Atmos. Environ., 254, 118349, https://doi.org/10.1016/j.atmosenv.2021.118349, 2021.

Zhang, Y., Soerensen, A. L., Schartup, A. T., and Sunderland, E. M.: A global model for methylmercury formation and uptake at the base of marine food webs, Global Biogeochem. Cycles, 34, e2019GB006348, https://doi.org/10.1029/2019GB006348, 2020.

Zhang, Y., Song, Z., Huang, S., Zhang, P., Peng, Y., Wu, P., Gu, J., Dutkiewicz, S., Zhang, H., Wu, S., Wang, F., Chen, L., Wang, S., and Li, P.: Global health effects of future atmospheric mercury emissions, Nat. Commun., 12, 3035, https://doi.org/10.1038/s41467-021-23391-7, 2021.

Zhou, C., Cohen, M. D., Crimmins, B. A., Zhou, H., Johnson, T. A., Hopke, P. K., and Holsen, T. M.: Mercury temporal trends in top predator fish of the Laurentian Great Lakes from 2004 to 2015: Are concentrations still decreasing?, Environ. Sci. Technol., 51, 7386–7394, https://doi.org/10.1021/acs.est.7b00982, 2017.

Zhou, X., He, T., Yin, Y., Jiang, T., Wu, P., Liu, J., Wang, Y., Yin, D., Liu, E., Ma, S., and Xie, Q.: Elevated methylmercury production in seasonally inundated sediments: Insights from DOM molecular composition, J. Hazard. Mater., 487, 137095, https://doi.org/10.1016/j.jhazmat.2025.137095, 2025.

Zhu, S., Zhang, Z., and Žagar, D.: Mercury transport and fate models in aquatic systems: A review and synthesis, Sci. Total Environ., 639, 538–549, https://doi.org/10.1016/j.scitotenv.2018.04.397, 2018.